Copy 6
RM E53G24

NACA RM E53G24

RESEARCH MEMORANDUM

PERFORMANCE OF AN ANNULAR TURBOJET COMBUSTOR HAVING REDUCED PRESSURE LOSSES AND USING PROPANE FUEL

By Carl T. Norgren and J. Howard Childs

Lewis Flight Propulsion Laboratory
Cleveland, Ohio

NATIONAL ADVISORY COMMITTEE
FOR AERONAUTICS

WASHINGTON

September 24, 1953

NACA RM E53G24

NATIONAL ADVISORY COMMITTEE FOR AERONAUTICS

RESEARCH MEMORANDUM

PERFORMANCE OF AN ANNULAR TURBOJET COMBUSTOR HAVING REDUCED PRESSURE LOSSES AND USING PROPANE FUEL

By Carl T. Norgren and J. Howard Childs

SUMMARY

An investigation was conducted to develop a high-combustion-efficiency turbojet combustor having pressure losses typical of those encountered in current turbojet engines. The investigation utilized (1) a previously developed 25.5-inch-diameter annular combustor with satisfactory pressure losses but low combustion efficiencies and (2) design principles evolved from tests in a combustor with high pressure loss and high combustion efficiency. Propane fuel was used to simulate vaporized jet fuel; the combustor design did not incorporate a vaporizer. A total of 13 air-entry hole modifications was investigated to obtain a combustor design that gave high combustion efficiencies and a satisfactory outlet radial temperature profile. The following results were obtained for simulated flight operation of a current turbojet engine with a compression ratio of 5.2 operating at a Mach number of 0.6 and 85 percent of rated speed (cruise).

The combustor giving the highest combustion efficiencies (model 28I) produced efficiencies above 95 percent at altitudes up to 71,500 feet with a combustor total-pressure loss of 4 to 6 percent of the combustor-inlet total pressure. At 56,000 feet the air mass-flow rate was increased 69 percent, and no appreciable effect on combustion efficiencies was noted; however, the combustor-inlet total-pressure loss increased to 11 to 15 percent of the combustor total pressure. The combustor-outlet radial temperature profile was in general satisfactory.

The results obtained indicate that combustor pressure losses in excess of 14 reference dynamic heads are not required to produce the air-flow patterns and turbulence necessary for high combustion efficiency. It was, however, much more difficult to control the combustor-outlet temperature profile to the desired pattern in the reduced-pressure-drop combustor than in high-pressure-drop combustors.

INTRODUCTION

As part of a general research program to improve turbojet combustor performance, an investigation was conducted at the NACA Lewis laboratory

with an annular combustor combining design features to obtain high combustion efficiency, reduced pressure losses, and a satisfactory outlet radial temperature profile.

It is shown in reference 1 that high-altitude performance of an annular experimental combustor is better with a vapor-fuel injection system than with a conventional liquid-fuel injection system. The high-combustion-efficiency combustor (model 14I) developed with vapor fuel (ref. 2) produced a total-pressure loss of 7.7 to 11.5 percent of the combustor-inlet total pressure. At the present time a total-pressure loss of 4 to 6 percent is typical in production-model turbojet combustors. The experimental combustor was redesigned in the investigation reported in reference 2 to obtain a pressure loss of 4 to 7.5 percent (model 15I). Although the combustion efficiency was reduced as a result of the design change, the data indicate that the injection of additional air into the primary zone would increase the combustion efficiency of model 15I.

Since a reduction in the pressure losses within the combustor will result in higher over-all cycle efficiency, the object of the investigation reported herein is to develop a combustor combining the high combustion efficiencies of model 14I with the lower pressure losses of model 15I. The design techniques employed included (1) alterations of the air-entry holes near the upstream end of model 15I combustor liner in order to admit more air into the primary zone, and (2) limited modification in the distribution of the remaining air to provide a satisfactory outlet radial temperature profile.

The investigation was conducted in a one-quarter segment of a 25.5-inch-diameter annular turbojet combustor installed in a direct-connect duct. In order to obtain data representative of the performance of the combustor with a fuel vaporizer installed, gaseous propane fuel was used throughout the investigation, on the assumption that the basic combustion properties of propane (e.g., flame speed and ignition energy) were sufficiently like those of vaporized jet fuel to make this substitution. A total of 13 combustor air-entry hole patterns was investigated. The operating conditions included low inlet-air pressures with air-flow rates typical of current engine design practice and 69 percent above current practice. Data presented include combustion efficiencies, combustor-outlet temperature profiles, and pressure losses over a range of fuel-air ratios. The performance data are compared with similar data for the combustors of reference 2. The final combustor performance is presented in terms of simulated flight operation in a current low-pressure-ratio turbojet engine.

APPARATUS

Installation

The combustor installation (fig. 1) was similar to that of reference 1. The combustor-inlet and combustor-outlet ducts were connected to the laboratory air supply and low-pressure exhaust systems, respectively. Air-flow rates and combustor pressures were regulated by remote-controlled valves located upstream and downstream of the combustor. The desired combustor-inlet air temperature was obtained by means of an electric air preheater.

Instrumentation

Air flow was metered by a concentric-hole, sharp-edge orifice installed according to A.S.M.E. specifications. The vapor fuel-flow rate was metered by a calibrated sharp-edge orifice. Thermocouples and pressure tubes were located at the combustor-inlet and outlet stations indicated in figure 1. The number, type, and position of these instruments at each of the three stations are indicated in figure 2. The combustor-outlet thermocouples and outlet total-pressure probes were located at centers of equal areas in the duct. Manifolded upstream total-pressure probes (station 1) and downstream static-pressure probes (station 3) were connected to absolute manometers; individual downstream total- and static-pressure probes were connected to banks of differential manometers. The chromel-alumel thermocouples (station 2) were connected to a self-balancing recording potentiometer.

The fuel used in this investigation was vaporized commercial propane supplied from the laboratory distribution system.

Combustors

A total of 13 combustor configurations was investigated. Each combustor consisted of a one-quarter segment (90°) of a single-annular combustor having an outside diameter of 25.5 inches, an inside diameter of 10.6 inches, and a length from fuel injectors to combustor-outlet thermocouples (station 2) of approximately 25 inches. The maximum combustor cross-sectional area was 105 square inches (corresponding to 420 sq in. for the complete combustor). A longitudinal cross-sectional view of the combustor is shown in figure 3, and a three-quarter cutaway view with the final liner configuration in figure 4.

Each combustor was given a numerical designation to indicate the liner configuration, followed by a letter designating the fuel injector design. Five equally spaced 7/64-inch orifices (corresponding to 20 orifices in the complete combustor) injected the propane fuel downstream

from the primary zone (injector modification I, ref. 2). Additional fuel injectors were located between these injectors for the purpose of supplying the higher fuel-flow rates required for low-altitude operation. No provision for vaporizing fuel was incorporated in the combustors.

Combustor design modifications included primary-zone modifications to improve the combustion efficiency, in conjunction with minor secondary-zone modifications to improve the radial outlet-temperature profile. (The upstream half of the combustor will be referred to as the primary zone, and the second half as the secondary zone.) The combustor air-entry hole configurations are given in figure 5. Each successive modification is shown in heavy solid lines, while the previous combustor pattern is indicated by dashed lines. Line cross-hatching indicates that an opening was closed. The investigation was conducted with combustor model 15I (from ref. 2 and reproduced in fig. 5(a)) as the original combustor configuration.

The design modifications investigated are listed in table I. An enlarged view of the final combustor (model 28I) is shown in figure 6.

PROCEDURE

Three performance characteristics desired of a turbojet combustor are a satisfactory outlet-temperature profile, a low pressure drop, and high combustion efficiency; the combustor design changes reported herein were made to obtain the best combination of these characteristics. Outlet radial temperature profiles were varied by opening or closing the secondary air slots so as to admit more or less cooling air. It was also attempted to obtain the maximum possible open hole area to reduce pressure drop.

Combustion efficiency was controlled by primary-zone modifications. As an aid in determining in advance the effect of primary-zone changes, additional air was injected into the primary combustion zone through the nonoperating fuel injectors. The effect of additional primary air on combustion efficiency was noted, and subsequent air-entry hole modifications were made accordingly.

Test Conditions

Combustion efficiency and combustor total-pressure-loss data were recorded for a range of fuel-air ratios at the following conditions:

Test condition	Combustor-inlet total pressure, P_i, in. Hg abs	Combustor-inlet total temperature, T_i, $^{\circ}F$	Air-flow rate per unit area,[1] W_a/A_r, lb/(sec)(sq ft)	Simulated flight altitude in reference engine at cruise speed, ft
A	15	268	2.14	56,000
B	8	268	1.14	70,000
C	5	268	.714	80,000
E	15	268	3.62	56,000

[1]Based on maximum combustor cross-sectional area.

These conditions simulate operation of the combustor in a reference turbojet engine with a 5.2 pressure ratio operating at a Mach number of 0.6. The cruise speed of the engine was assumed to be 85 percent of the rated rotor speed. Test conditions A through C required air-flow rates per unit combustor area that are typical of current turbojet engines. Test condition E required an air-flow rate that is 69 percent above current practice.

Calculations

Combustion efficiency was computed by the method of reference 3 as the percentage ratio of actual to theoretical increase in enthalpy from the combustor-inlet to the combustor-outlet instrumentation plane (station 1 to station 2). The arithmetic mean of the 30 outlet thermocouple indications was used to obtain the value of combustor-outlet enthalpy for the experimental combustor configurations. For the final combustor (model 28I) correction was made for variations in mass flow past each thermocouple indication of station 2. No corrections were made for radiation or velocity effects on the thermocouple indications.

The radial temperature distribution at the combustor outlet was determined for an outlet temperature rise of approximately 1180° F, which corresponds to the required value at 100 percent of rated engine speed in the reference turbojet engine at altitudes above the tropopause. The temperature at each of five radial positions was computed as the average of four thermocouple readings at each position (see fig. 2(b)). The temperature rake at each side wall of the combustor was not included in these average temperatures, since the side walls exert an influence on the flow pattern and temperature profile that would not be present in a complete combustor annulus.

The total-pressure loss was computed as the dimensionless ratio of the total-pressure loss to the combustor reference dynamic pressure and

to the combustor total pressure. Combustor reference velocities were computed from the air mass-flow rate, the combustor-inlet density, and the maximum combustor cross-sectional area (105 sq in.).

RESULTS AND DISCUSSION

The experimental data obtained with the 13 combustor configurations investigated are presented in table II. A list of all symbols is presented in the appendix.

Combustor Development

Combustion efficiency. - Combustion efficiency is presented in figure 7 over a range of fuel-air ratios at various test conditions for the experimental combustor models 16I to 28I. Figure 8 gives a comparison of the combustion efficiencies of the experimental combustors at test condition C for two temperature-rise values (from fig. 7). Temperature-rise values of 680° and 1180° F were selected, since they represent turbine temperature requirements of the reference turbojet engine operating above the tropopause at 85 and 100 percent of rated speed, respectively. Model 28I combustor, which was selected as the best combustor from this group, operated at the highest combustion efficiency at the higher temperature-rise level (fig. 8).

Combustor-outlet temperature profiles. - In figure 9 the radial temperature profiles for several combustor models are shown. The original configuration, model 15I (ref. 2), is included for comparison. In model 23I the inner-wall open area had been increased 25 percent and the outer wall area decreased 12 percent from model 15I before the more symmetrical radial profile shown in figure 9 was obtained. A further 10-percent area increase in the inner wall and a 20-percent decrease in the outer wall resulted in but slight improvement of the radial temperature profile (model 26I, fig. 9). For the low-pressure-drop combustors used in this investigation, the combustor-outlet temperature profile was, therefore, relatively insensitive to changes in the liner air-entry holes. In an earlier investigation with combustors having a higher pressure drop (ref. 1), the effect of changes in liner air-entry holes on temperature profile was much more pronounced.

Performance of Model 28I

The following results were obtained with combustor model 28I, which was considered to have the best performance characteristics of the configurations investigated. A comparison of model 28I is made with the previously developed combustors of reference 2.

Combustion efficiency. - In figure 10(a) are presented the values of combustion efficiency obtained with model 28I combustor over a range of fuel-air ratios at each of three inlet pressures (test conditions A, B, and C). Similar data are shown in figure 10(b) for constant inlet pressure and the two air-flow rates investigated. These curves have been corrected for mass-flow distribution. Shown also, for comparison, are the corresponding uncorrected curves from figure 7. It is noted that correcting for distribution reduced the computed combustion efficiency. Previous experience (ref. 2) indicates that uneven temperature profiles generally cause erroneously high arithmetically averaged temperature readings. The corrected combustion efficiency at condition A is observed to be 102.5 percent. It is believed that this erroneous result could be attributed to inaccurate average outlet-temperature determination, to cumulative errors in fuel and air metering systems, or both.

3008

Reproducibility tests for model 28I were not made; however, duplicate data that were recorded at test conditions B and E for model 24I are indicated by solid symbols in figure 7(f). Data at test condition B were obtained with the original model 24I and with a duplicate model 24I rebuilt from model 25I combustor. Duplicate data at test condition E were obtained at the beginning and at the end of the test program with the model 24I combustor. The data show an average deviation of less than ± 1.5 percent. Since neither warping of the combustor liner nor any apparent changes in alinement occurred during the entire experimental program, this reproducibility is believed to be applicable to model 28I.

In figure 11 combustor model 28I is compared with the combustors (models 14I and 15I) of reference 2 at test condition C. Model 14I represents the previously developed combustor attaining the highest efficiency at severe operating conditions. A specialized vapor-fuel system as well as primary-zone modifications were incorporated in the design to obtain this performance with vapor fuel; however, the pressure loss through the combustor was high. Lower pressure losses in model 15I resulted from alterations of the combustor walls of model 14I so as to obtain a larger flow passage between the liner and combustor housing, as discussed in reference 2. Although the air-entry hole pattern for model 15I was similar to that of model 14I, the lower pressure loss of model 15I resulted in a reproportioning of the air; a greater portion of the air entered the combustor near the downstream end and caused the combustor primary zone to operate fuel-rich. The marked decrease in efficiency with increase in fuel-air ratio shown for model 15I in figure 11 is typical of the performance of combustors having a fuel-rich primary zone. As was pointed out in reference 2, additional air-injection into the primary zone of model 15I combustor improved the combustion efficiency. Thirteen combustor modifications were required to translate this known requirement effectively into the final combustor design (model 28I). Figure 11 shows that the model 28I combustor was developed to operate with efficiencies comparable to model 14I combustor of reference 2.

[redacted]

Combustor-outlet temperature profiles. - The temperature profile of the final combustor configuration is shown in figure 12. The temperature distribution is considered acceptable in that the individual temperatures deviated by no more than $\pm 200^{\circ}$ F from the desired temperature at any radial position. The maximum temperature, however, occurred at 60 percent rather than at the normally desired 85 percent of the blade height, which indicates that a moderately hot core of exhaust gas is present in the combustor that is not adequately dispersed by the air entering the secondary slots.

Pressure losses. - The pressure losses through combustor model 28I are presented in figure 13. The dimensionless ratio of the total-pressure loss to the reference dynamic pressure $\Delta P/q_r$ is presented as a function of the density ratio ρ_1/ρ_2 in figure 13(a) for model 28I combustor. The pressure-loss data of combustor models 14I and 15I are included for comparison. This figure shows that the isothermal (no heat addition) pressure loss was 50 percent less in combustor model 28I than in model 14I. As was noted previously, these models operated with comparable combustion efficiency. The observed decrease in pressure loss was primarily due to a redesign of the combustor walls, as discussed in reference 2. Model 28I, with 16 percent greater air-entry hole area than model 15I, had a pressure drop approximately 15 percent below that of model 15I. The isothermal pressure drop ($\Delta P/q_r = 14$) obtained with model 28I compares favorably with current production-model combustors.

The pressure-drop data of figure 13(a) are replotted in figure 13(b) to indicate the loss in percentage of combustor-inlet total pressure. It is shown that a 4- to 6-percent total-pressure loss (due to heat addition plus frictional losses occurring through the combustor) is encountered with velocities typical of current design practice. As the combustor air flow is increased to 69 percent above conventional practice, the combustor pressure losses increase to 11 to 15 percent of the combustor-inlet total pressure.

Significance of results to engine performance. - The combustion efficiencies of model 28I combustor are plotted in figure 14 as a function of $V_r/p_i T_i$ (ref. 4). The data points were selected from figures 9 and 10 for two values of combustor temperature rise, 680° and 1180° F, which correspond to operation in the reference turbojet engine at 85 and 100 percent of rated speed, respectively. The curves are drawn through the data points representing standard combustor velocity conditions (test conditions A, B. and C); however, the data symbols are also included to indicate efficiencies at the higher reference velocity (condition E).

[redacted]

The difference of approximately $3\frac{1}{2}$ percent between the two curves of figure 14 indicates that the combustion efficiency remained relatively constant over the range of fuel-air ratios required in actual engine operation.

Figure 15, which presents the estimated combustion efficiency of the combustor at various flight conditions in the reference turbojet engine, was obtained from the correlation curves of figure 14 by the method of reference 5. The two included data points indicate the efficiency obtained at the equivalent simulated operating conditions. The curves of figure 15 show that the combustor should be expected to operate at efficiencies above 95 percent up to an altitude of 71,500 feet at cruise (85-percent rated) engine speed.

For the reference turbojet engine, approximately 0.7-percent decrease in thrust may be expected from a 1-percent loss in total pressure in the combustor (assuming constant efficiency of engine components). Thus, the reduction in total-pressure loss from model 14I to model 28I would effect an increase of 2.5 to 5.0 percent in thrust in the reference turbojet engine.

SUMMARY OF RESULTS

In the investigation reported herein, an annular turbojet combustor having a high efficiency and conventional pressure losses was developed for high-altitude operation by means of air-entry hole modifications. The combustor was operated with propane to simulate vaporized jet fuel; a vaporizer was not incorporated in the design. In the following results the performance values quoted for simulated flight performance correspond to the final combustor design in a current 5.2-pressure-ratio turbojet engine at a flight Mach number of 0.6:

1. A combustor (model 28I) was developed which combined high combustion efficiency with pressure losses of only 4 to 6 percent of the combustor-inlet total pressure at velocities representative of current engine design practice. The combustion efficiency was above 95 percent at simulated altitudes up to 71,500 feet at 85 percent of rated speed.

2. At 56,000 feet and 85-percent rated speed, no appreciable effect on combustion efficiency resulted from increasing the air-flow rate to a value of 69 percent above current design practice. At the increased velocity, however, the combustor total-pressure drop was 11 to 15 percent of the combustor-inlet total pressure.

3. The combustor-outlet temperature profile was generally satisfactory for the final combustor design.

[redacted]

4. The combustor with a reduced pressure drop [$\Delta P/q_r$ (total-pressure loss/reference dynamic pressure) = 14] developed in this investigation produced approximately the same combustion efficiencies as a high-pressure-drop combustor ($\Delta P/q_r$ = 28) reported previously.

CONCLUDING REMARKS

After it had been established that additional air-entry holes near the upstream end of the liner were required for higher combustion efficiency, a total of 13 air-entry hole modifications were necessary before the desired result was achieved. Therefore, even when general combustor design principles are known, considerable tailoring of minor design features may be required in order to exploit these principles correctly.

It was much more difficult to control the combustor-outlet temperature profile to the desired pattern in the reduced-pressure-drop combustor than in high-pressure-drop combustors. It was shown that combustor pressure losses in excess of $\Delta P/q_r$ = 14 are not required to produce the air-flow patterns and turbulence necessary for high combustion efficiency. The possibility of reducing pressure losses further below $\Delta P/q_r$ = 14 has not been investigated.

Lewis Flight Propulsion Laboratory
National Advisory Committee for Aeronautics
Cleveland, Ohio, July 29, 1953

APPENDIX - SYMBOLS

The following symbols are used in this report:

A	area, sq ft
f	fuel-air ratio, lb/lb
P	combustor-inlet total pressure, in. Hg abs
ΔP	total-pressure drop through combustor, in. Hg
p	static pressure, lb/sq ft abs
q	dynamic pressure, in. Hg
T	combustor total temperature, $^{\circ}R$
ΔT	mean temperature rise through combustor, $^{\circ}F$
V	combustor velocity, ft/sec
W	flow rate, lb/sec
η	efficiency, percent
ρ	density, lb/cu ft

Subscripts:

a	air
b	burner
f	fuel
i	inlet
o	outlet
r	reference
1,2,3	instrumentation stations

REFERENCES

1. Norgren, Carl T., and Childs, J. Howard: Effect of Liner Air-Entry Holes, Fuel State, and Combustor Size on Performance of an Annular Turbojet Combustor at Low Pressures and High Air-Flow Rates. NACA RM E52J09, 1953.

2. Norgren, Carl T., and Childs, J. Howard: Effect of Fuel Injectors and Liner Design on Performance of an Annular Turbojet Combustor With Vapor Fuel. NACA RM E53B04, 1953.

3. Turner, L. Richard, and Bogart, Donald: Constant-Pressure Combustion Charts Including Effects of Diluent Addition. NACA Rep. 937, 1949. (Supersedes NACA TN's 1086 and 1655.)

4. Childs, J. Howard: Preliminary Correlation of Efficiency of Aircraft Gas-Turbine Combustors for Different Operating Conditions. NACA RM E50F15, 1950.

5. Olson, Walter T., Childs, J. Howard, and Scull, Wilfred E.: Method for Estimating Combustion Efficiency at Altitude Flight Conditions from Combustor Tests at Unrelated Conditions. NACA RM E53F17, 1953.

[redacted]

TABLE I. - DESIGN MODIFICATIONS

Model number	Description of change	Modification reference to figure 5
16I	Radiation shield made removable; annular space around radiation shield set at two positions, 1/16 and 1/8 in.	(b)
17I	Primary holes behind radiation shield doubled in number and top secondary slots opened	(c)
18I	Primary holes enlarged from 11/64-in. diam. to 3/8-in. diam.	(d)
19I	Primary holes enlarged from 21/64-in. diam. to 5/8-in. diam.	(e)
20I	Continuous primary inlet-air scoops added; model 19I modification voided	(f)
21I	Radiation-shield annular space sealed	(f)
22I	Radiation-shield annular space reset and drilled to admit air directly into primary zone; bottom secondary slots opened	(g)
23I	Primary holes enlarged from 11/64-in. diam. to 5/16-in. diam.; top secondary slots blocked and bottom secondary slots opened	(h)
24I	Primary holes enlarged from 11/64-in. diam. to 1/4-in. diam.; bottom secondary slots opened	(i)
25I	Primary holes enlarged from 1/4-in. diam. to 5/16-in. diam.	(j)
26I	Primary holes relocated and top secondary slots blocked	(k)
27I	Primary holes enlarged from 21/64-in. diam. to 3/8-in. diam.	(l)
28I	Primary holes blocked	(m) and figure 6

TABLE II. - EXPERIMENTAL RESULTS

Combustor-inlet total pressure, P_1, in. Hg	Combustor-inlet total temperature, T_1, °R	Air-flow rate, w_a, lb/sec	Combustor reference velocity, V_r, ft/sec	Fuel-flow rate, W_f, lb/hr	Fuel-air ratio, f	Mean combustor-outlet temperature, T_o, °R	Mean temperature rise through combustor, ΔT, °R	Combustion efficiency, η_b, percent	Total-pressure drop through combustor, ΔP, in. Hg	Combustion parameter, V_r/P_1T_1, ft, lb, sec, °R units
Model 16I ($\frac{1}{16}$-in. annulus)										
5.0	731	0.522	81.3	18.8	0.0100	1310	579	74.8	0.30	323×10^{-6}
↓	728	.522	81.0	24.4	.0129	1430	702	71.3	.30	323
	731	.522	81.3	29.2	.0155	1538	807	69.3	.33	325
	729	.522	81.1	35.2	.0187	1640	911	66.0	.35	323
	728	.522	81.0	41.7	.0222	1740	1012	62.8	.33	323
5.1	728	.522	79.4	41.7	.0222	1780	1052	65.4	.33	310
5.0	725	.522	80.6	41.7	.0222	1670	945	58.4	.33	323
8.0	731	.829	80.6	28.0	.00940	1340	609	84.0	.40	199
↓	726	.826	79.8	36.3	.0122	1495	769	83.0	.43	199
	727	.834	80.6	54.6	.0182	1795	1068	80.2	.51	201
	726	.825	79.7	70.8	.0238	2010	1284	75.7	.56	198
Model 16I ($\frac{1}{8}$-in. annulus)										
8.0	729	0.830	80.5	----	--------	----	----	----	----	200×10^{-6}
5.0	725	.525	81.1	----	--------	----	----	----	----	324
↓	731	.525	81.8	14.1	0.00749	1160	429	73.1	0.24	325
	729	.528	81.7	23.6	.0124	1390	661	69.6	.28	325
	733	.525	82.0	31.0	.0164	1570	837	68.4	.31	324
↓	732	.525	81.8	37.1	.0196	1635	903	62.6	.31	324
8.0	720	.835	80.0	19.6	.00652	1160	440	85.8	.35	201
↓	716	.830	79.0	32.1	.0107	1410	694	84.3	.40	200
	724	.835	80.4	38.4	.0127	1530	806	83.5	.43	201
	727	.832	80.5	44.7	.0149	1640	913	82.0	.48	200
	729	.836	81.1	52.1	.0173	1760	1031	81.0	.48	201
↓	722	.827	79.5	60.2	.0202	1920	1198	82.0	.52	199
Model 17I										
5.0	722	0.523	80.4	20.2	0.0107	1335	613	74.3	0.27	323×10^{-6}
↓	725	.524	80.9	23.8	.0126	1430	705	73.4	.25	324
5.05	727	.523	80.2	28.7	.0152	1550	823	72.0	.29	317
5.0	724	.523	80.7	33.2	.0176	1615	891	68.2	.31	323
5.1	722	.521	78.6	41.5	.0221	1835	1113	69.6	.33	309
5.0	726	.521	80.6	41.6	.0221	1590	864	53.3	.31	322
8.0	724	.822	79.1	34.3	.0116	1470	746	84.5	.40	198
↓	728	.827	80.1	52.9	.0177	1785	1057	81.2	.47	198
Model 18I										
5.0	732	0.521	81.2	20.4	0.0108	1350	618	74.0	0.27	322×10^{-6}
↓	724	.522	80.6	23.5	.0125	1430	706	74.1	.27	322
	728	.520	80.7	26.5	.0141	1515	787	73.8	.28	322
	722	.521	80.2	34.6	.0184	1650	928	68.1	.30	322
	722	.522	80.4	44.7	.0238	1660	938	54.3	.31	322
↓	726	.522	80.8	41.9	.0222	1810	1084	67.3	.33	322
7.95	732	.838	82.1	23.8	.0079	1265	533	86.7	.36	204
8.0	729	.836	81.1	37.5	.0124	1520	791	83.8	.41	201
8.05	730	.841	81.1	46.7	.0154	1680	950	82.9	.45	200
8.0	728	.836	80.9	64.7	.0215	1910	1182	76.3	.50	201
Model 19I										
5.0	723	0.524	80.7	17.4	0.00926	1195	972	65.5	0.23	324×10^{-6}
↓	729	.521	80.9	23.4	.0124	1395	666	70.1	.27	322
	729	.523	81.2	28.3	.0150	1520	791	70.0	.30	323
↓	729	.522	81.1	37.2	.0197	1630	901	62.0	.31	323
5.1	724	.521	78.7	58.8	.0313	1980	1256	57.4	.35	309
8.0	728	.839	81.2	27.4	.0090	1290	562	80.0	.37	202
↓	730	.851	82.6	34.8	.0113	1455	725	83.8	.41	205
	727	.846	81.7	54.9	.0180	1810	1083	82.0	.48	203

NACA

[redacted]

TABLE II. - EXPERIMENTAL RESULTS - Continued

Combustor-inlet total pressure, P_1, in. Hg	Combustor-inlet total temperature, T_1, °R	Air-flow rate, W_a, lb/sec	Combustor reference velocity, V_r, ft/sec	Fuel-flow rate, W_f, lb/hr	Fuel-air ratio, f	Mean combustor-outlet temperature, T_o, °R	Mean temperature rise through combustor, ΔT, °F	Combustion efficiency, η_b, percent	Total-pressure drop through combustor, ΔP, in. Hg	Combustion parameter, V_r/P_1T_1, ft, lb, sec, °R units
Model 20I										
5.0	730	0.522	81.3	20.4	0.0111	1320	590	69.0	----	--------
|	728	.521	80.7	24.0	.0128	1410	682	70.0	----	--------
|	728	.522	81.2	27.4	.0146	1460	732	66.5	----	--------
|	725	.522	81.0	34.9	.0181	1460	735	56.7	----	--------
↓	728	.561	80.7	34.4	.0170	1570	842	67.6	----	--------
8.0	728	.832	80.6	24.3	.0081	1260	532	84.4	----	--------
|	724	.832	80.4	31.2	.0104	1390	666	84.0	----	--------
|	726	.830	80.2	37.5	.0125	1510	784	83.3	----	--------
↓	726	.832	80.0	43.5	.0145	1630	904	83.0	----	--------
Model 21I										
15.0	730	2.64	145	69.9	0.0074	1260	530	92.3	2.16	203×10^{-6}
15.1	726	2.66	145	85.0	.0089	1365	639	92.3	2.30	206
15.0	723	2.66	145	102.3	.0107	1480	757	92.5	2.45	208
15.1	726	2.66	145	119.5	.0125	1560	834	88.9	2.55	206
5.0	723	.522	80.2	18.1	.0096	1255	532	71.5	----	--------
5.1	721	.521	79.8	25.4	.0136	1470	749	73.1	----	--------
5.1	726	.521	80.0	22.2	.0118	1380	654	72.6	----	--------
↑	730	.521	80.0	32.2	.0172	1540	810	63.6	----	--------
5.2	726	.521	80.0	32.2	.0172	1625	899	70.8	----	--------
5.1	722	.521	80.0	53.2	.0289	1970	1208	62.3	----	--------
5.5	721	.531	------	17.8	.0093	1300	579	80.2	----	--------
5.4	724	.522	------	19.3	.0102	1360	636	80.4	----	--------
|	722	.521	------	23.6	.0125	1455	733	76.8	----	--------
|	726	.521	------	29.8	.0159	1570	844	71.1	----	--------
|	722	.527	------	34.5	.0182	1700	978	73.0	----	--------
|	727	.520	------	48.0	.0256	1780	1053	57.3	----	--------
|	723	.520	------	48.0	.0256	1630	908	48.9	----	--------
↓	721	.520	------	19.0	.0101	1330	609	77.7	----	--------
8.4	729	.830	------	28.7	.0096	1365	636	85.9	----	--------
↑	723	.833	------	48.7	.0162	1720	997	83.0	----	--------
5.4	721	.524	------	17.7	.0094	1320	599	82.4	----	--------
|	727	.525	------	21.0	.0111	1400	673	79.2	----	--------
|	726	.524	------	25.4	.0134	1540	814	80.2	----	--------
↓	730	.524	------	30.5	.0162	1635	905	75.2	----	--------
5.14	730	.521	78.7	35.5	.0189	1760	1030	74.4	0.25	304
5.7	732	.521	------	42.6	.0227	1910	1178	72.3	----	--------
↑	735	.520	------	42.7	.0228	1960	1225	75.1	----	--------
5.6	724	.520	------	23.0	.0122	1470	746	80.0	----	--------
7.88	732	.823	81.7	28.8	.0096	1390	658	88.4	.37	205
8.3	725	.826	------	38.3	.0129	1590	865	89.1	----	--------
7.95	732	.826	80.9	57.3	.0192	1910	1178	84.3	.48	201
8.0	734	.821	------	19.5	.0066	1173	441	84.9	----	--------
Model 22I										
5.4	727	0.519	------	18.7	0.00898	1310	583	83.9	----	--------
5.35	730	.518	------	21.5	.0115	1430	700	79.7	----	--------
5.4	732	.517	------	26.2	.0140	1560	828	78.4	----	--------
5.35	732	.517	------	33.5	.0180	1680	948	71.4	----	--------
5.4	727	.517	------	45.1	.0242	1800	1073	61.5	----	--------
|	725	.517	------	45.1	.0242	1900	1175	67.8	----	--------
↓	725	.517	------	45.1	.0242	1920	1195	69.0	----	--------
8.4	725	.837	------	32.4	.0107	1470	745	90.6	----	--------
Model 23I										
5.4	726	0.518	------	15.6	0.00837	1250	524	80.5	----	--------
5.45	724	.517	------	19.1	.0102	1400	676	85.8	----	--------
5.4	727	.519	------	24.6	.0132	1550	823	82.8	----	--------
|	728	.514	------	29.2	.0158	1680	952	81.2	----	--------
|	728	.516	------	33.5	.0180	1765	1037	78.3	----	--------
|	730	.515	------	41.2	.0222	1900	1170	73.1	----	--------
↓	730	.516	------	41.3	.0222	1915	1185	74.1	----	--------
8.08	724	.836	79.50	----	------	----	----	----	----	196×10^{-6}
8.35	728	.838	------	27.4	.00908	1390	662	94.7	----	--------
8.3	725	.826	------	17.6	.00594	1135	410	87.5	----	--------

TABLE II. - EXPERIMENTAL RESULTS - Continued

Combustor-inlet total pressure, P_1, in. Hg	Combustor-inlet total temperature, T_1, °R	Air-flow rate, W_a, lb/sec	Combustor reference velocity, V_r, ft/sec	Fuel-flow rate, W_f, lb/hr	Fuel-air ratio, f	Mean combustor-outlet temperature, T_o, °R	Mean temperature rise through combustor, ΔT, °F	Combustion efficiency, η_b, percent	Total-pressure drop through combustor, ΔP, in. Hg	Combustion parameter, V_r/p_1T_1, ft, lb, sec, °R units
Model 23I (continued)										
8.25	728	0.831	------	33.0	0.0110	1510	782	93.2	----	--------
8.3	725	.830	------	38.0	.0127	1625	900	94.1	----	--------
↓	726	.838	77.93	44.0	.0145	1745	1019	94.1	0.40	$187X10^{-6}$
↓	725	.828	------	50.6	.0169	1865	1140	91.1	----	--------
15.3	726	2.61	------	69.9	.0074	1275	549	94.9	----	--------
15.15	720	2.63	------	87.5	.0092	1435	715	100.9	----	--------
15.2	719	2.66	------	102.0	.0106	1540	821	101.1	----	--------
↑	728	2.64	------	123.0	.0129	1670	942	96.9	----	--------
15.15	720	2.64	------	143.0	.0150	1770	1050	94.0	----	--------
15.1	725	2.65	------	159.0	.0167	1845	1120	91.2	----	--------
Model 24I										
5.3	734	0.523	77.06	-----	------	734	0	------	----	$286X10^{-6}$
8.3	724	.832	77.17	-----	------	724	0	------	----	186
5.2	722	.523	------	14.8	0.0078	1245	523	85.3	----	--------
5.25	724	.524	------	18.5	.0098	1410	686	90.8	----	--------
5.2	723	.524	77.62	22.6	.0119	1533	810	89.4	0.25	299
5.25	724	.523	------	28.7	.0152	1700	976	86.1	----	--------
5.23	732	.523	77.98	33.5	.0177	1815	1083	83.3	.23	295
↑	726	.523	------	38.2	.0202	1910	1184	80.8	----	--------
8.3	723	.836	------	18.6	.0061	1175	452	93.0	----	--------
↓	728	.838	78.18	24.7	.0081	1340	612	96.4	.27	187
↓	730	.833	------	29.8	.0099	1485	755	99.5	----	--------
↓	728	.829	77.27	37.4	.0125	1660	932	99.1	.30	185
↑	730	.832	------	48.2	.0161	1870	1140	98.4	----	--------
5.3	722	.525	------	27.5	.0145	1600	878	80.4	----	--------
5.7	728	.523	------	43.5	.0231	1930	1202	72.6	----	--------
↑	722	.523	------	22.0	.0117	1460	738	82.9	----	--------
Model 25I										
8.3	728	0.834	------	22.1	0.0073	1200	472	81.8	----	--------
↓	726	.829	------	32.5	.0109	1490	764	92.1	----	--------
↓	726	.836	------	54.9	.0182	1910	1184	89.2	----	--------
Model 24I (reconstructed from 25I)										
15.1	730	2.64	------	60.5	0.0063	1180	450	90.2	----	--------
15.1	722	2.62	141.5	74.2	.0078	1315	593	97.2	1.685	$199X10^{-6}$
15.2	729	2.64	------	85.1	.0089	1405	676	98.3	----	--------
↓	720	2.65	------	97.1	.0101	1505	785	101.0	----	--------
↓	722	2.65	------	109.0	.0115	1590	868	99.8	----	--------
↓	728	2.63	------	123.0	.0129	1680	952	98.0	----	--------
14.8	728	2.04	------	52.2	.0070	1280	552	99.8	----	--------
15.0	720	2.01	------	65.2	.0089	1440	720	104.2	----	--------
15.2	731	1.99	------	76.0	.0105	1555	824	102.7	----	--------
↑	724	2.04	------	86.3	.0117	1640	916	103.7	----	--------
15.3	729	2.02	------	101.0	.0139	1795	1066	103.0	----	--------
↑	730	2.02	------	117.0	.0161	1910	1180	100.0	----	--------
15.2	733	1.55	------	37.2	.00664	1245	512	98.6	----	--------
↑	728	1.56	------	48.3	.00857	1430	702	106.4	----	--------
15.1	730	1.53	------	58.0	.0105	1585	855	107.1	----	--------
15.2	736	1.54	------	68.8	.0123	1710	974	105.4	----	--------
15.2	728	1.55	------	78.2	.0139	1810	1082	104.6	----	--------
↓	723	1.56	------	90.1	.0160	1930	1207	102.9	----	--------
↓	724	1.56	------	99.3	.0176	2025	1301	101.8	----	--------
15.3	728	1.55	------	109.0	.0194	2110	1382	98.9	----	--------
8.2	727	.852	------	24.3	.0079	1300	573	92.9	----	--------
↓	723	.849	------	28.7	.0094	1410	687	95.0	----	--------
↓	726	.851	------	33.3	.0108	1530	804	97.2	----	--------
↓	727	.851	------	37.9	.0123	1640	913	98.1	----	--------
↓	722	.840	------	44.0	.0145	1750	1028	95.2	----	--------
↓	724	.849	------	53.4	.0174	1935	1211	95.2	----	--------
↓	724	.842	------	62.8	.0207	2060	1336	90.0	----	--------
8.25	729	.845	------	70.1	.0230	2150	1421	87.1	----	--------
15.0	728	2.64	------	73.0	.0076	1335	607	102.1	----	--------
15.0	727	2.64	------	91.1	.0095	1450	723	98.7	----	--------
↓	727	2.65	------	107.0	.0112	1560	833	97.9	----	--------
↓	728	2.64	------	122.0	.0128	1660	932	96.9	----	--------
↓	728	2.64	------	139.0	.0146	1760	1032	95.3	----	--------
↓	730	2.63	------	169.0	.0178	1890	1160	89.2	----	--------
↓	729	2.63	144.0	198.0	.0208	2010	1281	85.4	----	--------
15.1	722	2.62	------	226.0	.0239	2090	1368	80.5	----	--------

TABLE II. - EXPERIMENTAL RESULTS - Concluded

Combustor-inlet total pressure, P_1, in. Hg	Combustor-inlet total temperature, T_1, °R	Air-flow rate, W_a, lb/sec	Combustor reference velocity, V_r, ft/sec	Fuel-flow rate, W_f, lb/hr	Fuel-air ratio, f	Mean combustor-outlet temperature, T_o, °R	Mean temperature rise through combustor, ΔT, °F	Combustion efficiency, η_b, percent	Total pressure drop through combustor, ΔP, in. Hg	Combustion parameter, V_r/p_1T_1, ft, lb, sec, °R units
	Model 26I									
5.2	730	0.521	80.4	19.1	0.0102	1365	635	81.5	----	--------
	728	.522	80.2	21.4	.0114	1450	722	83.2	----	--------
	722	.522	80.0	27.1	.0144	1620	898	83.2	----	--------
	729	.522	80.2	31.6	.0167	1750	1021	82.7	----	--------
↓	726	.522	80.1	37.8	.0201	1905	1179	80.7	----	--------
5.0	724	.522	80.1	42.5	.0228	2000	1276	78.3	----	--------
8.1	723	.833	80.1	24.4	.0081	1310	587	93.0	----	--------
8.0	726	.834	80.3	29.0	.0097	1410	684	92.2	----	--------
8.1	725	.834	80.2	32.2	.0107	1510	785	95.8	----	--------
8.1	726	.834	80.3	38.8	.0129	1660	934	96.5	----	--------
8.2	727	.833	80.3	44.3	.0148	1785	1058	97.0	----	--------
↑	726	.828	80.3	57.2	.0192	2010	1284	93.0	----	--------
	Model 27I									
5.0	724	0.522	80.1	18.6	0.0099	1315	591	77.8	----	--------
	724	.522	80.1	21.1	.0112	1420	696	81.2	----	--------
	726	.522	80.2	26.4	.0140	1605	879	83.4	----	--------
	722	.522	80.0	30.6	.0163	1700	978	81.2	----	--------
	726	.522	80.2	34.6	.0184	1800	1074	79.3	----	--------
↓	727	.522	80.2	41.0	.0219	1910	1183	75.0	----	--------
8.0	726	.829	79.8	29.4	.0099	1440	714	94.3	----	--------
	721	.831	79.8	37.2	.0124	1620	899	94.8	----	--------
↓	722	.831	79.9	42.3	.0142	1730	1008	95.0	----	--------
	Model 28I									
5.0	727	0.524	80.5	16.6	0.0087	1305	578	85.3	----	--------
	728	.524	80.6	21.2	.0113	1476	747	87.3	----	--------
	724	.524	80.3	24.9	.0132	1605	881	88.8	----	--------
	728	.524	80.5	28.4	.0156	1725	997	86.5	----	--------
	722	.524	80.4	32.8	.0174	1830	1108	87.1	----	--------
	722	.521	80.1	36.1	.0192	1895	1173	84.0	----	--------
↓	726	.563	80.2	36.1	.0179	1880	1154	88.0	----	--------
15.1	722	2.62	143.0	59.8	.0069	1240	518	102.8	----	--------
	723	2.65	143.0	79.2	.0083	1395	672	105.0	----	--------
	728	2.69	144.0	90.7	.0096	1510	782	107.0	----	--------
	728	2.64	144.0	107.0	.0113	1605	877	103.2	----	--------
	727	2.65	144.0	124.0	.0130	1705	978	100.5	----	--------
	725	2.66	144.0	148.0	.0155	1850	1125	98.5	----	--------
	720	2.64	143.0	164.0	.0172	1915	1195	92.0	----	--------
	724	1.57	80.2	54.8	.0062	1235	511	105.3	----	--------
	726	1.56	80.3	44.6	.0080	1380	654	106.2	----	--------
	728	1.55	80.4	53.5	.0096	1500	772	105.7	----	--------
	723	1.56	80.3	64.0	.0114	1640	917	107.2	----	--------
	728	1.57	80.4	73.0	.0129	1740	1012	108.2	----	--------
	726	1.57	80.3	80.3	.0142	1820	1094	104.0	----	--------
	730	1.57	80.5	88.5	.0157	1910	1180	103.0	----	--------
	727	1.56	80.4	100.	.0178	2030	1303	101.0	----	--------
5.0	724	.521	80.2	-----	-------	----	----	0	----	--------
8.0	722	.833	80.1	-----	-------	----	----	0	----	--------
	728	.835	80.4	18.2	.0061	1160	432	90.3	----	--------
	724	.835	80.2	29.4	.0098	1450	726	97.1	----	--------
	726	.835	80.3	34.3	.0114	1570	844	97.3	----	--------
	728	.835	80.4	39.2	.0131	1690	962	98.4	----	--------
	722	.835	80.1	44.7	.0149	1785	1063	99.6	----	--------
	721	.835	80.1	54.0	.0180	1945	1224	93.6	----	--------
↓	728	.835	80.4	61.5	.0205	2050	1322	87.5	----	--------
5.0	722	.522	79.4	35.9	.0191	1895	1173	83.7	0.30	303×10^{-6}
15.0	723	2.65	139.4	79.0	.0083	1395	672	102.9	2.07	201
	720	2.64	138.0	164.0	.0172	1915	1195	93.2	2.27	201
	726	1.56	79.7	45.7	.0079	1380	654	102.0	.75	100
↓	730	1.57	80.5	88.5	.0157	1910	1180	100.9	.77	100
5.0	729	.52	79.4	-----	-------	----	----	-----	.18	300
8.0	722	.83	79.0	-----	-------	----	----	-----	.30	187
15.0	728	2.64	79.7	-----	-------	----	----	-----	1.83	201

NACA

[redacted]

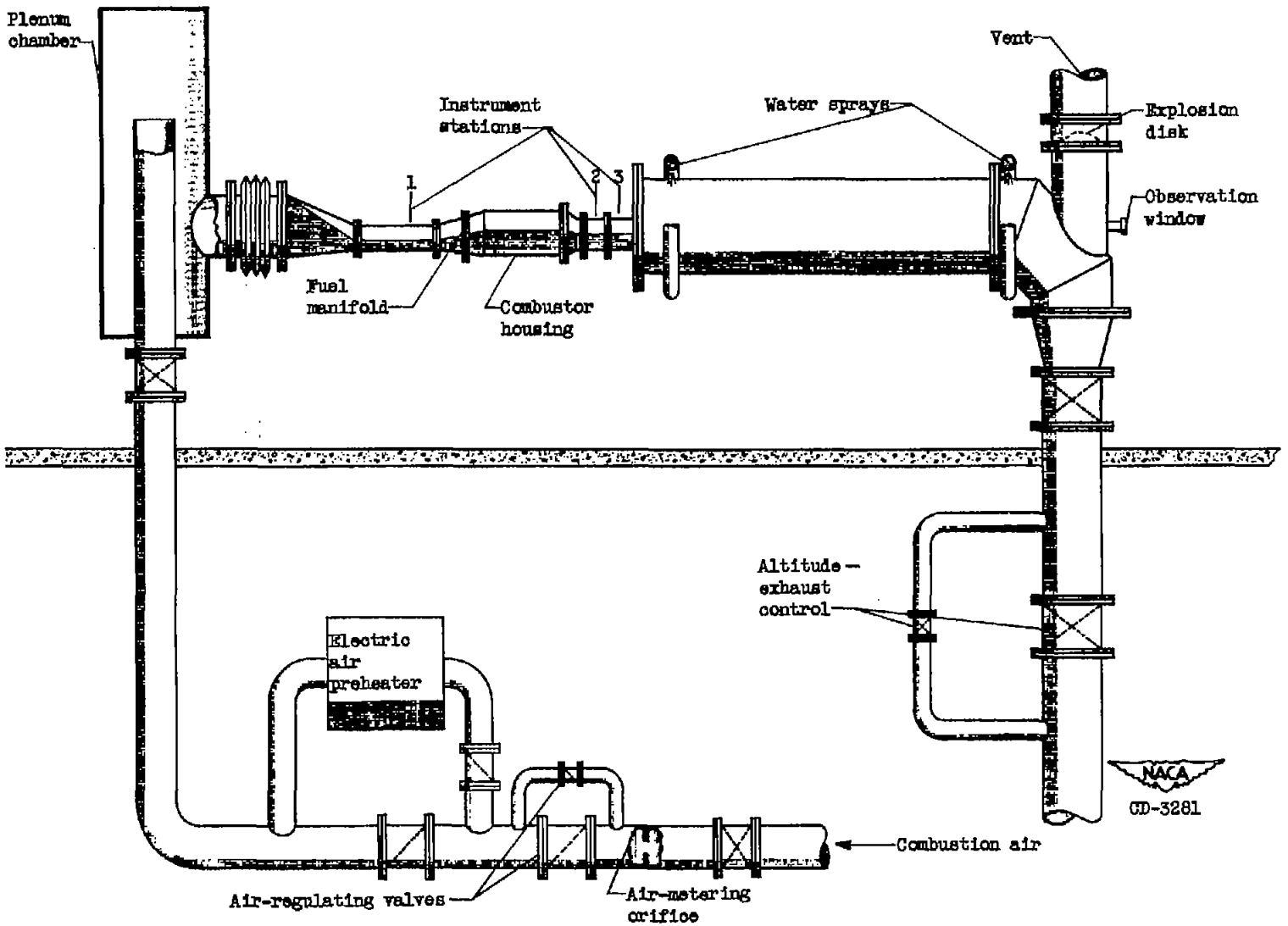

Figure 1. - Installation of one-quarter sector of 255-inch-diameter annular combustor.

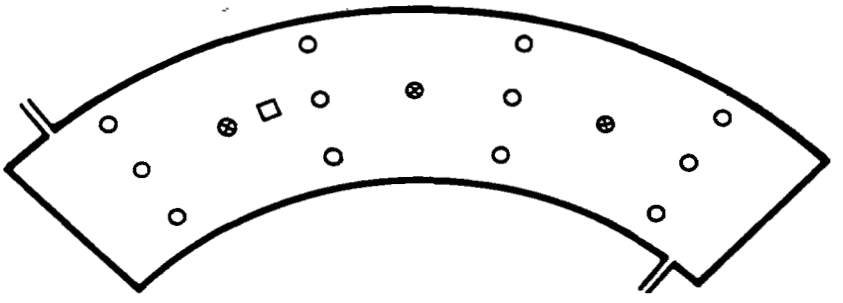

(a) Inlet thermocouples (iron constantan), inlet total-pressure rakes, and stream static probe at station 1.

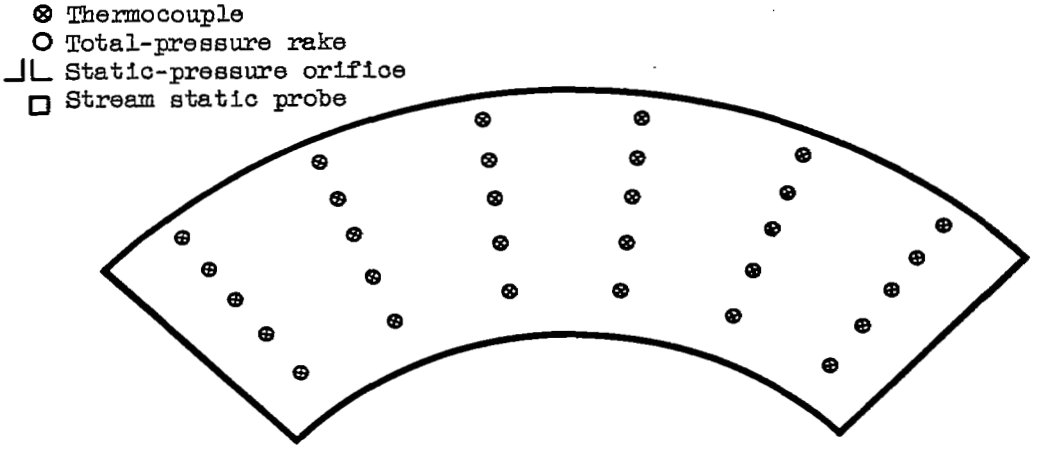

(b) Outlet thermocouples (chromel-alumel) at station 2.

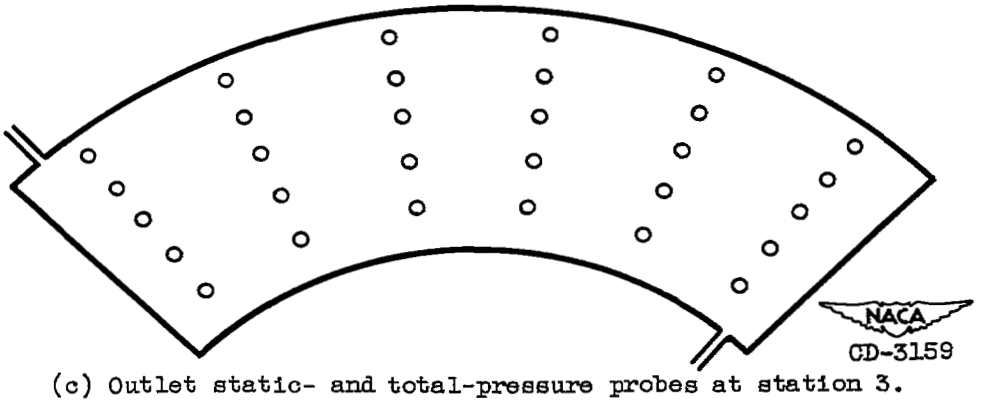

(c) Outlet static- and total-pressure probes at station 3.

Figure 2. - Location of combustor instrumentation.

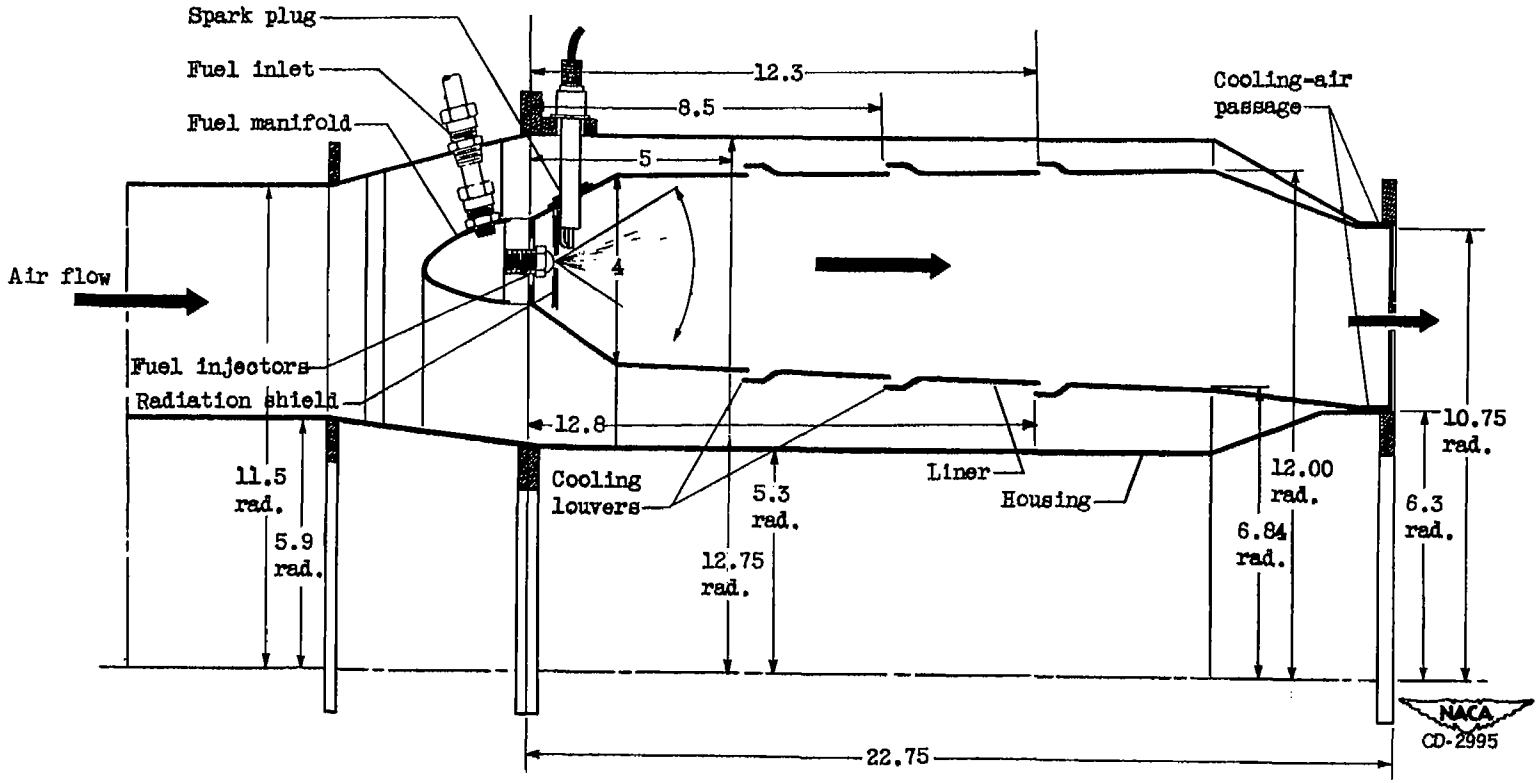

Figure 3. - Longitudinal cross-sectional view of experimental combustor. (Dimensions are in inches.)

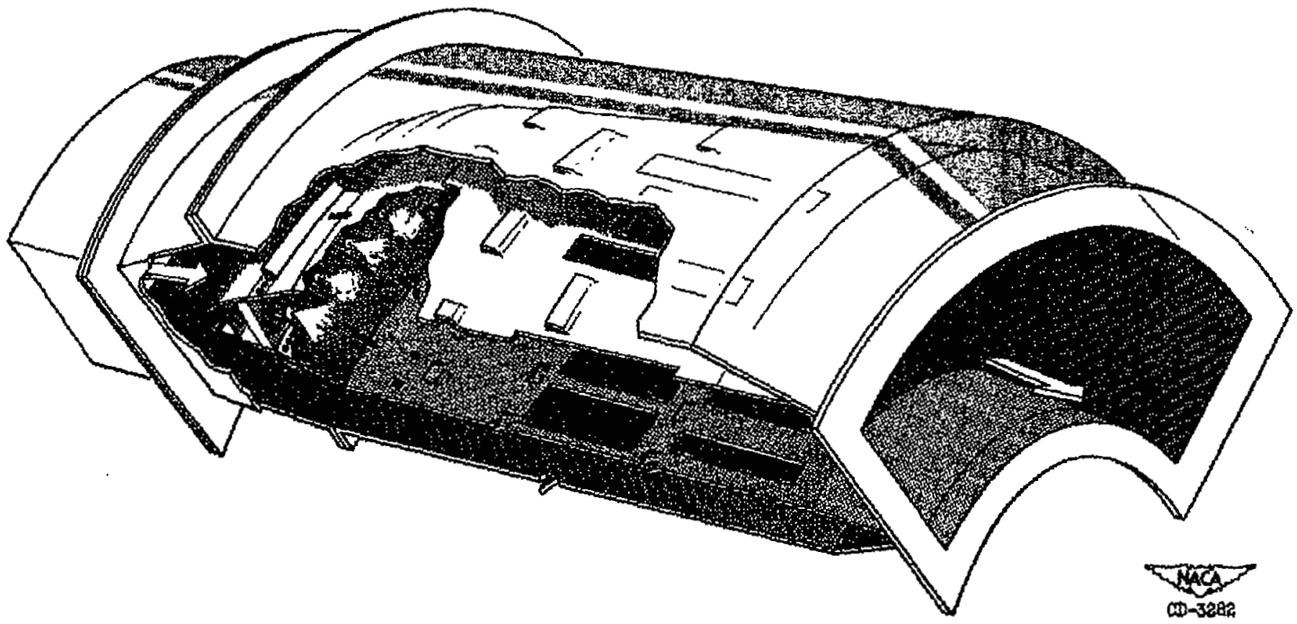

Figure 4. - One-quarter sector of model 28I annular combustor assembled in test ducting.

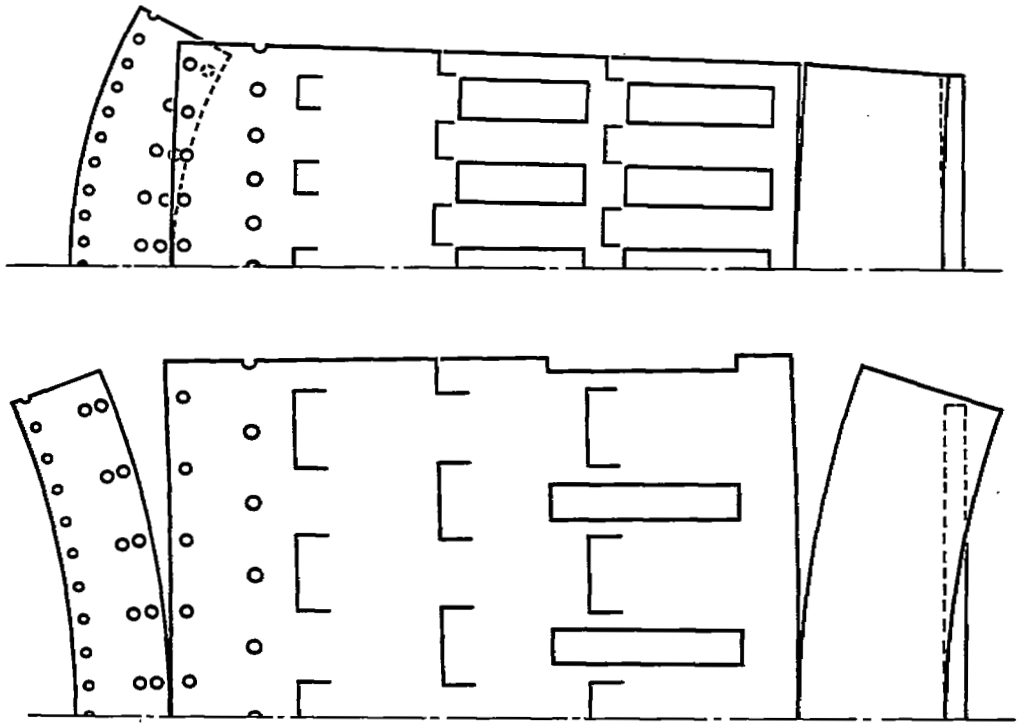

(a) Model 15I.

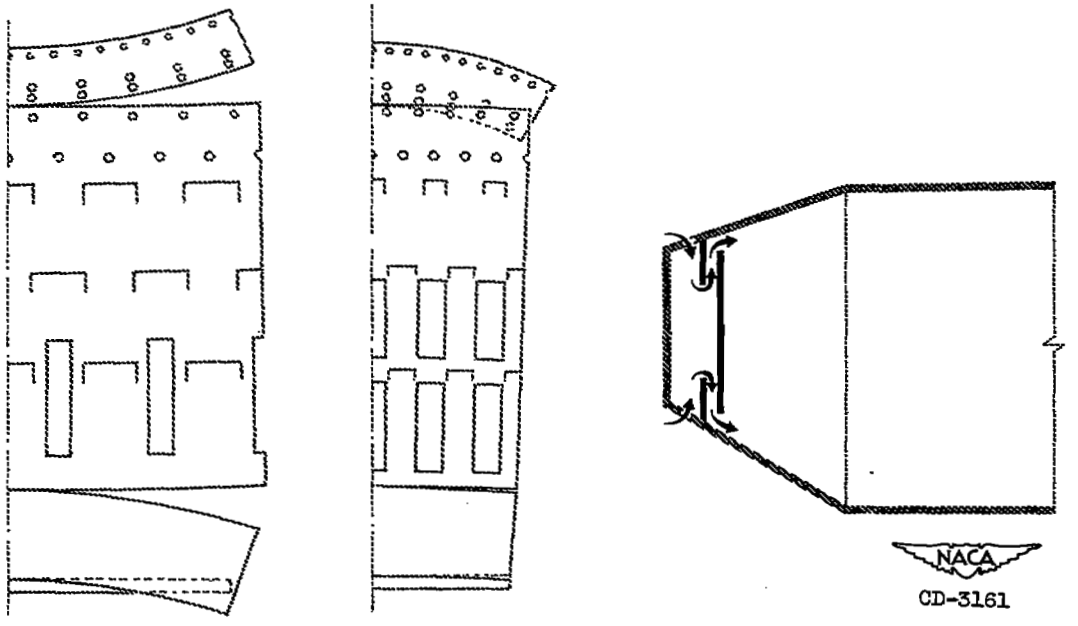

(b) Model 16I.

Figure 5. - Experimental combustor hole patterns.

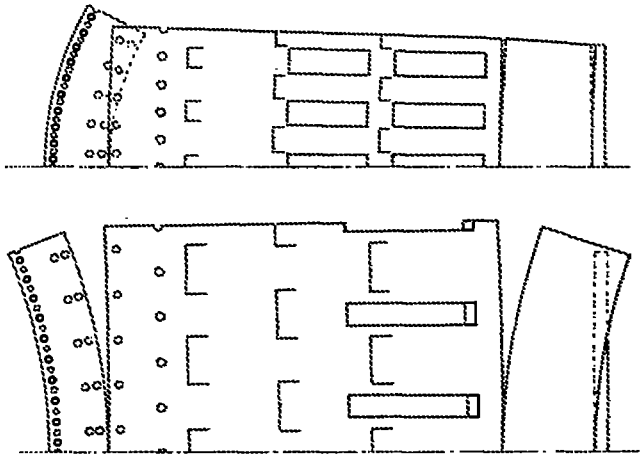

(c) Model 17I.

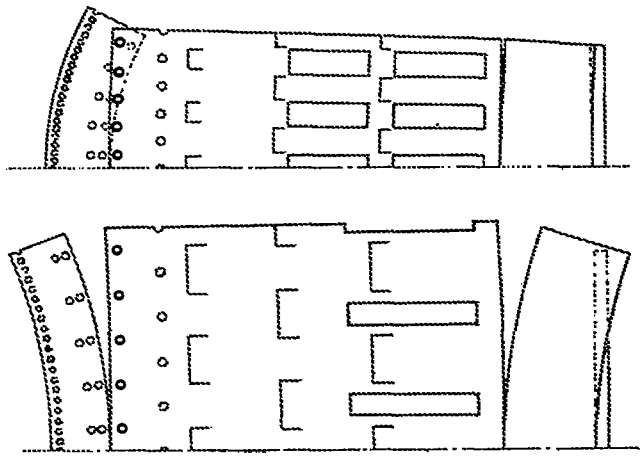

(d) Model 18I.

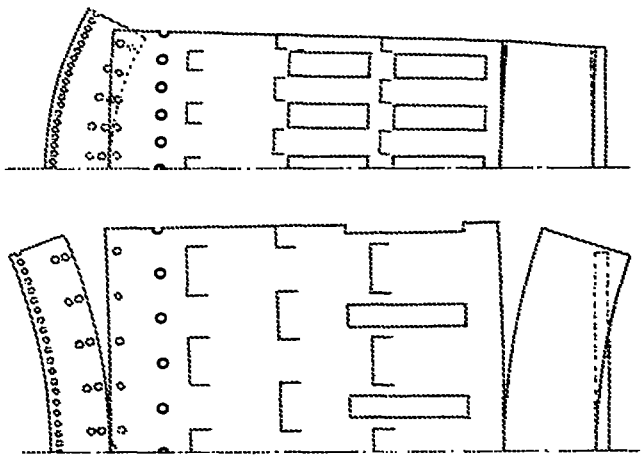

(e) Model 19I.

CD-3162

Figure 5. - Continued. Experimental combustor hole patterns.

[redacted]

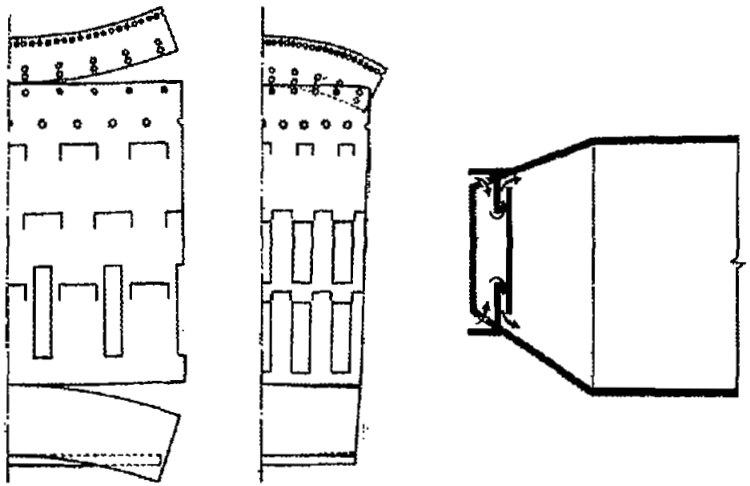

(f) Models 20I and 21I.

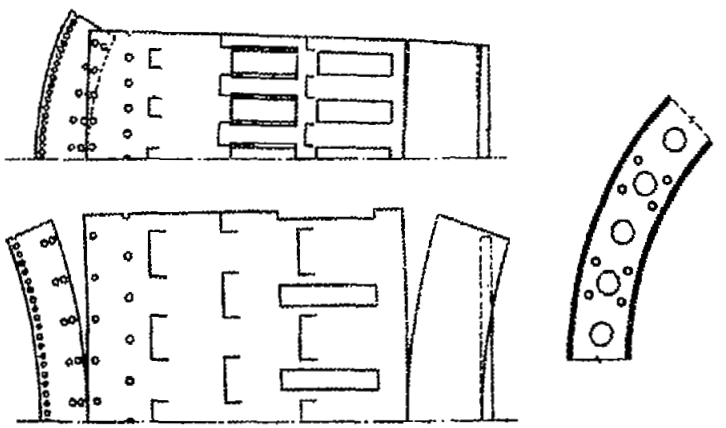

(g) Model 22I.

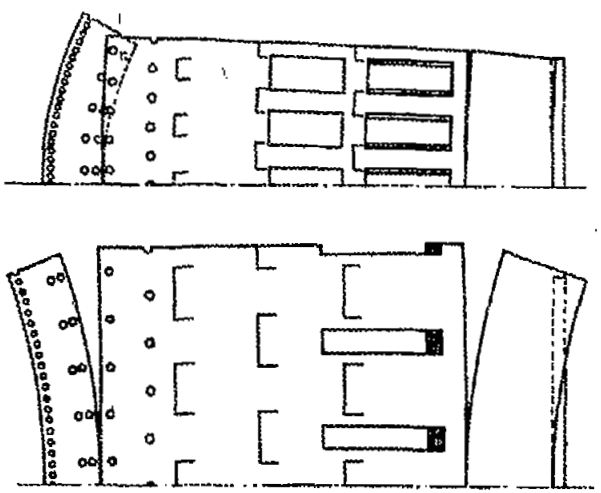

(h) Model 23I.

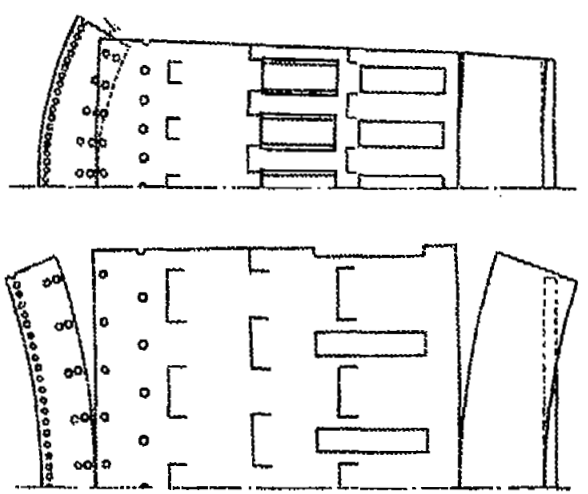

(i) Model 24I.

NACA
CD-3163
CD-3164

Figure 5. - Continued. Experimental combustor hole patterns.

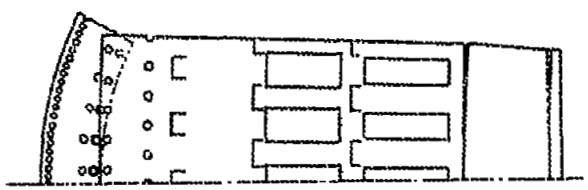

(j) Model 25I.

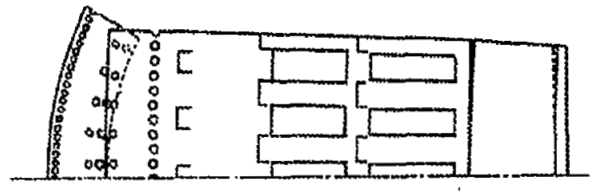

(k) Model 26I.

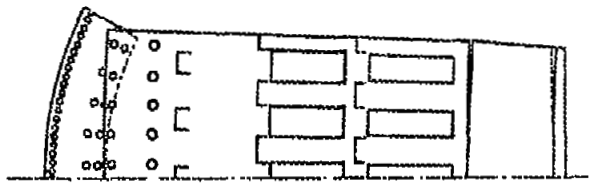

(l) Model 27I.

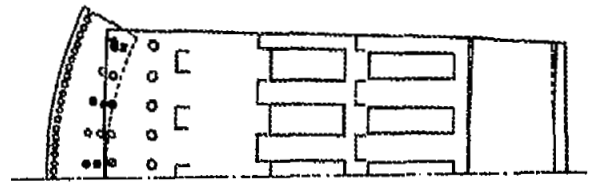

(m) Model 28I.

NACA
CD-3164
CD-3165

Figure 5. - Concluded. Experimental combustor hole patterns.

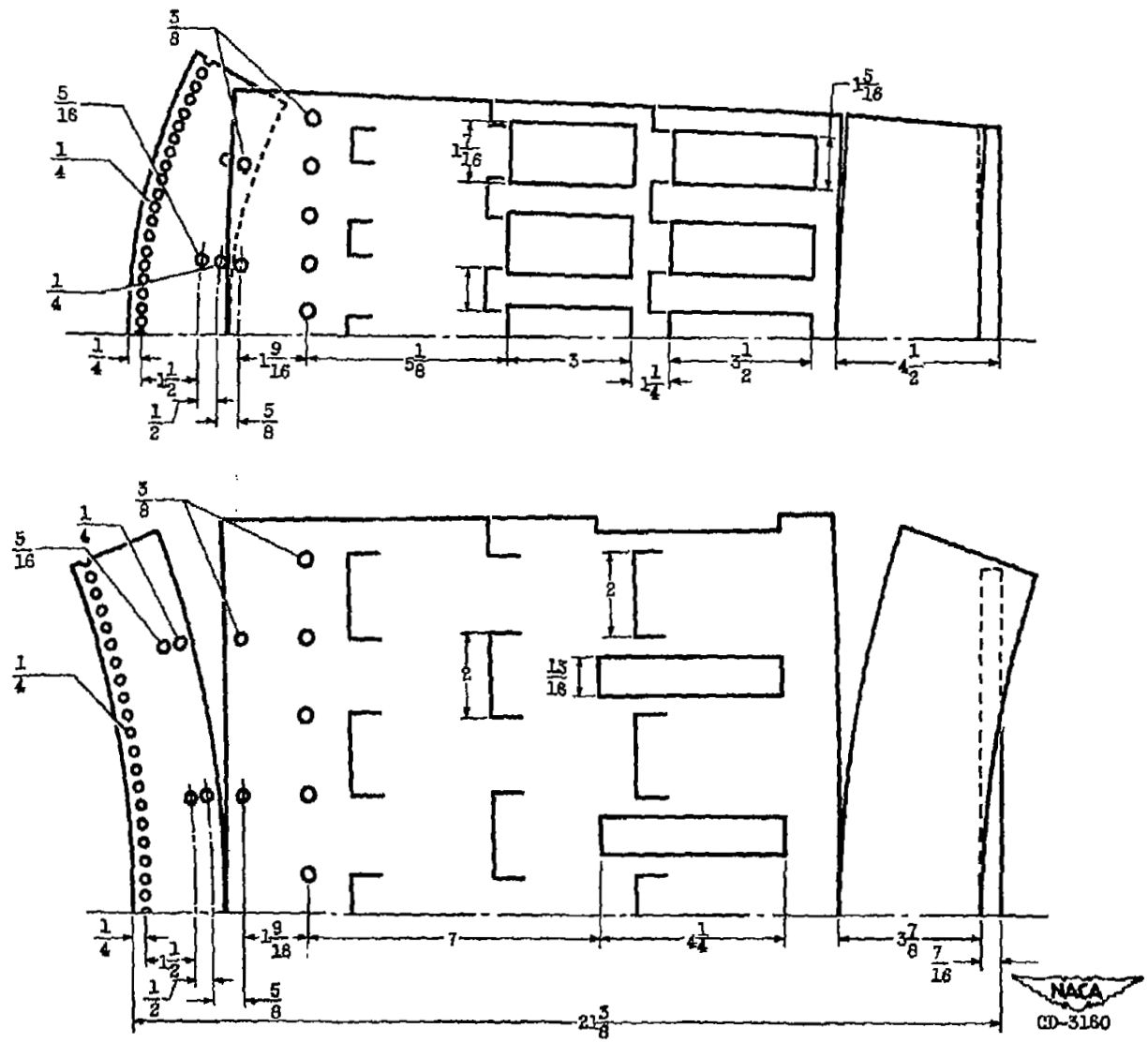

Figure 6. - Liner air-entry holes of model 28I combustor. (Dimensions are in inches.)

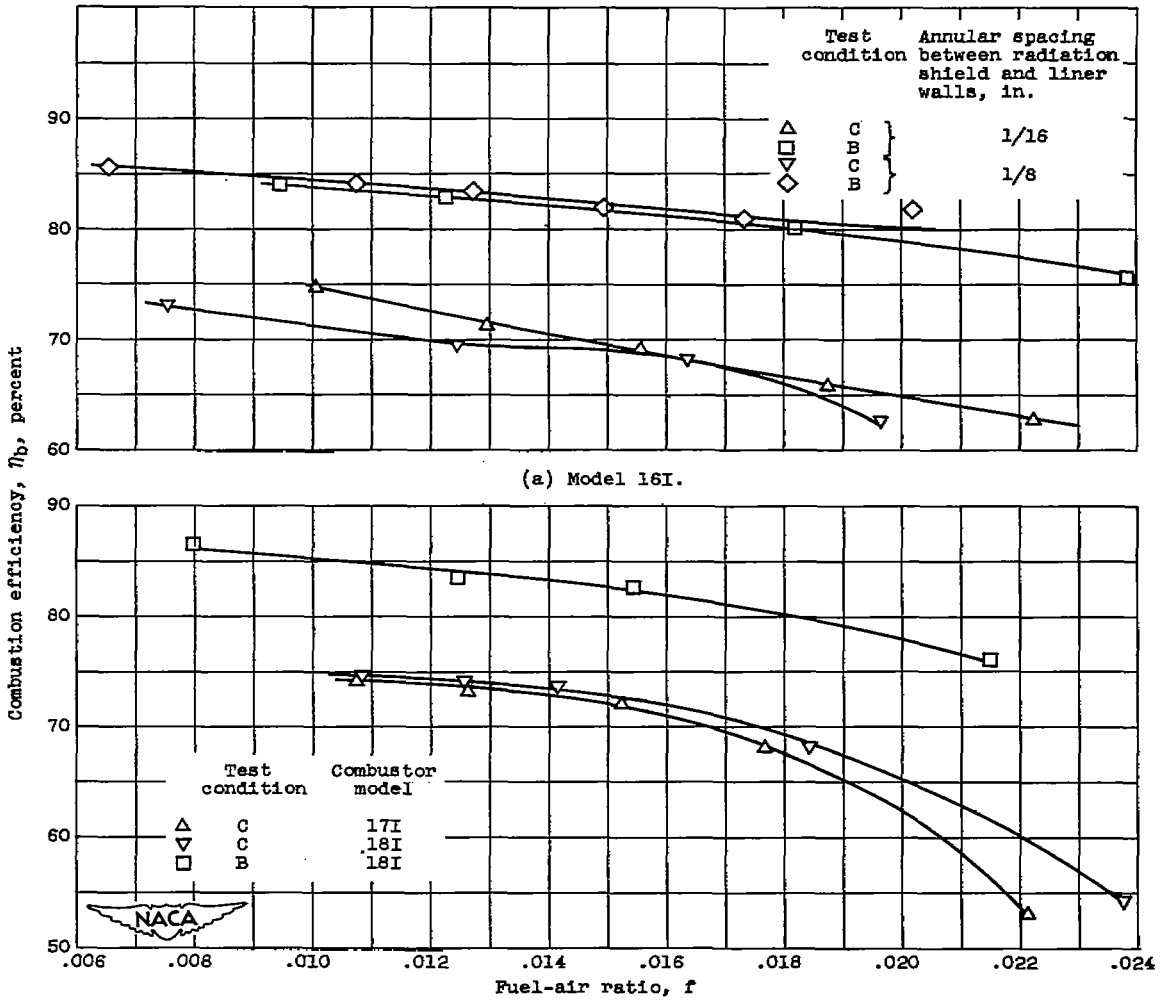

Figure 7. - Combustion efficiency of experimental combustor.

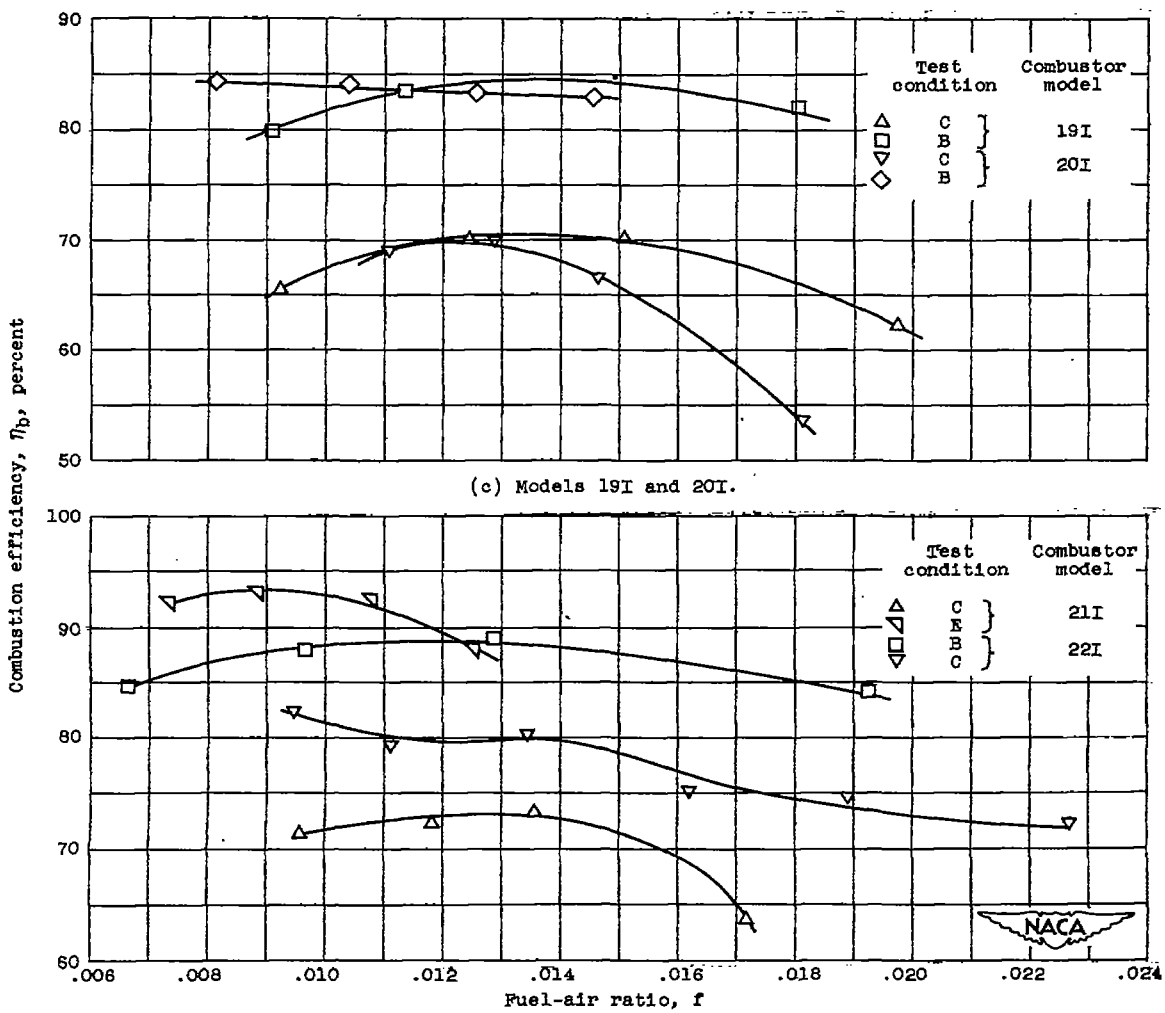

Figure 7. - Continued. Combustion efficiency of experimental combustor.

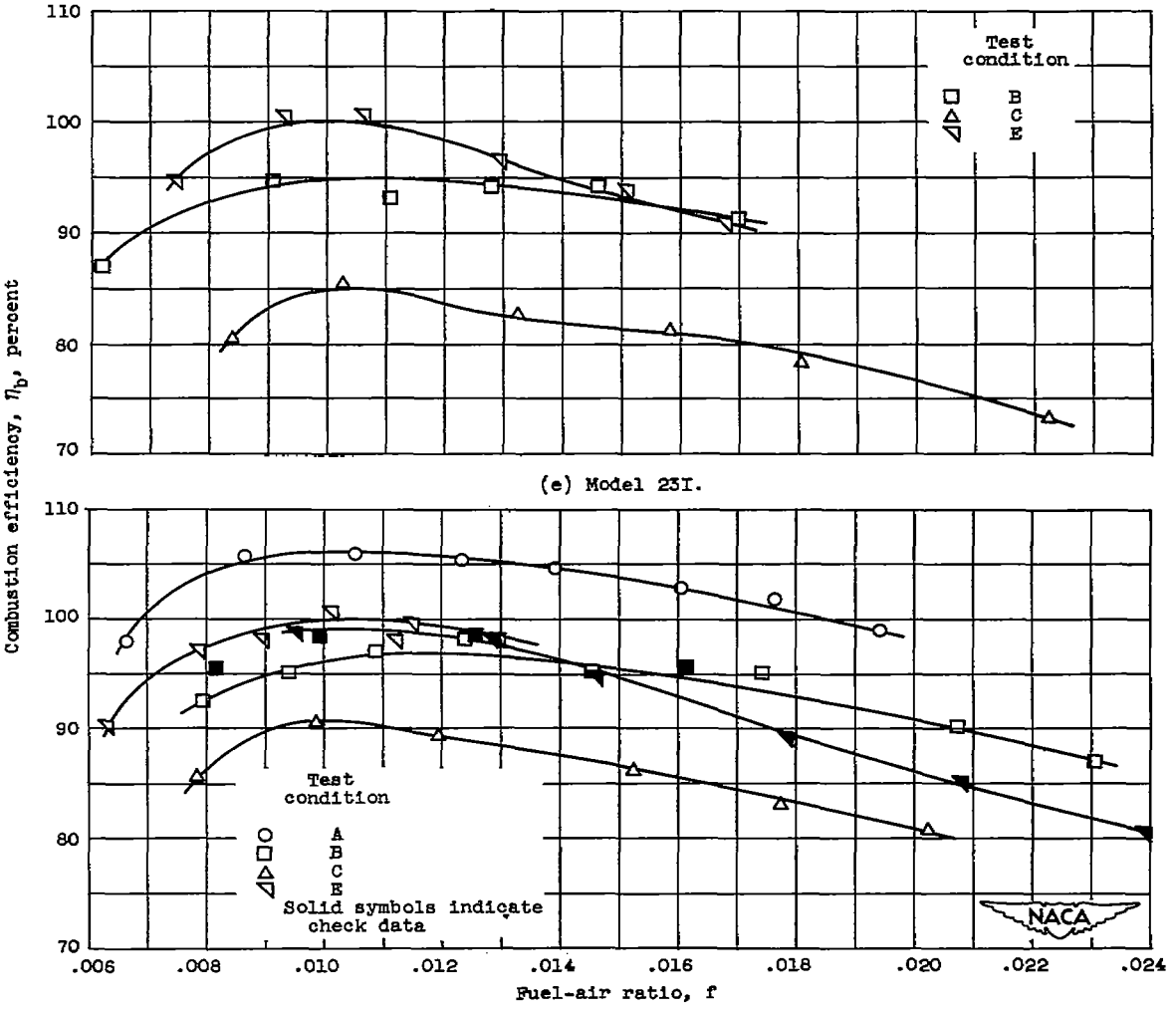

Figure 7. - Continued. Combustion efficiency of experimental combustor.

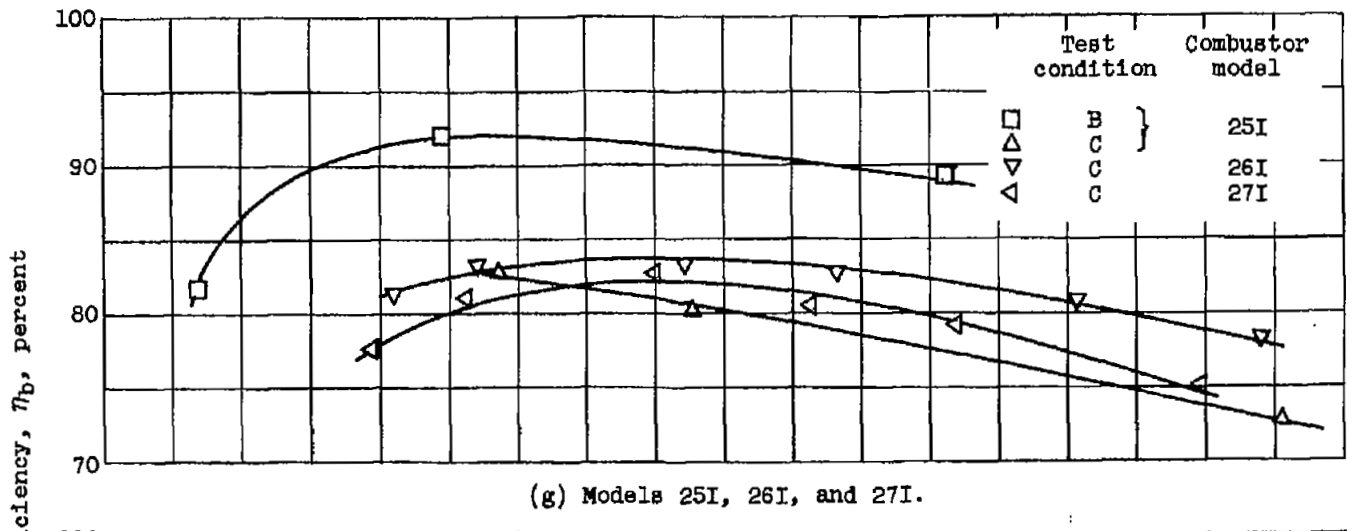

(g) Models 25I, 26I, and 27I.

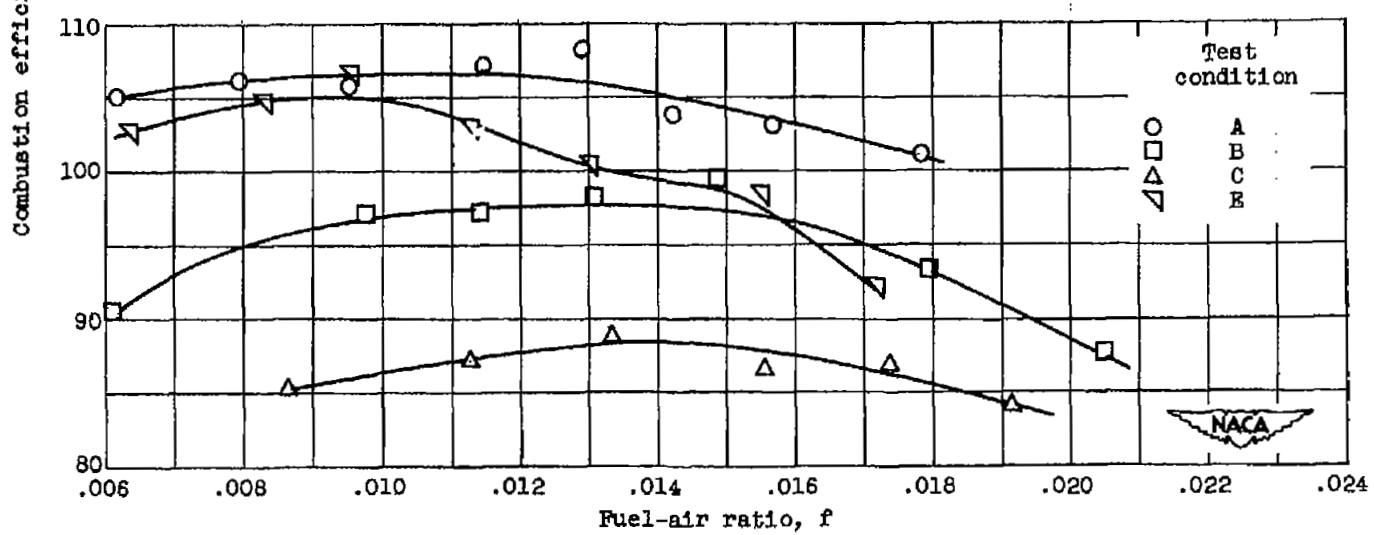

(h) Model 28I.

Figure 7. - Concluded. Combustion efficiency of experimental combustor.

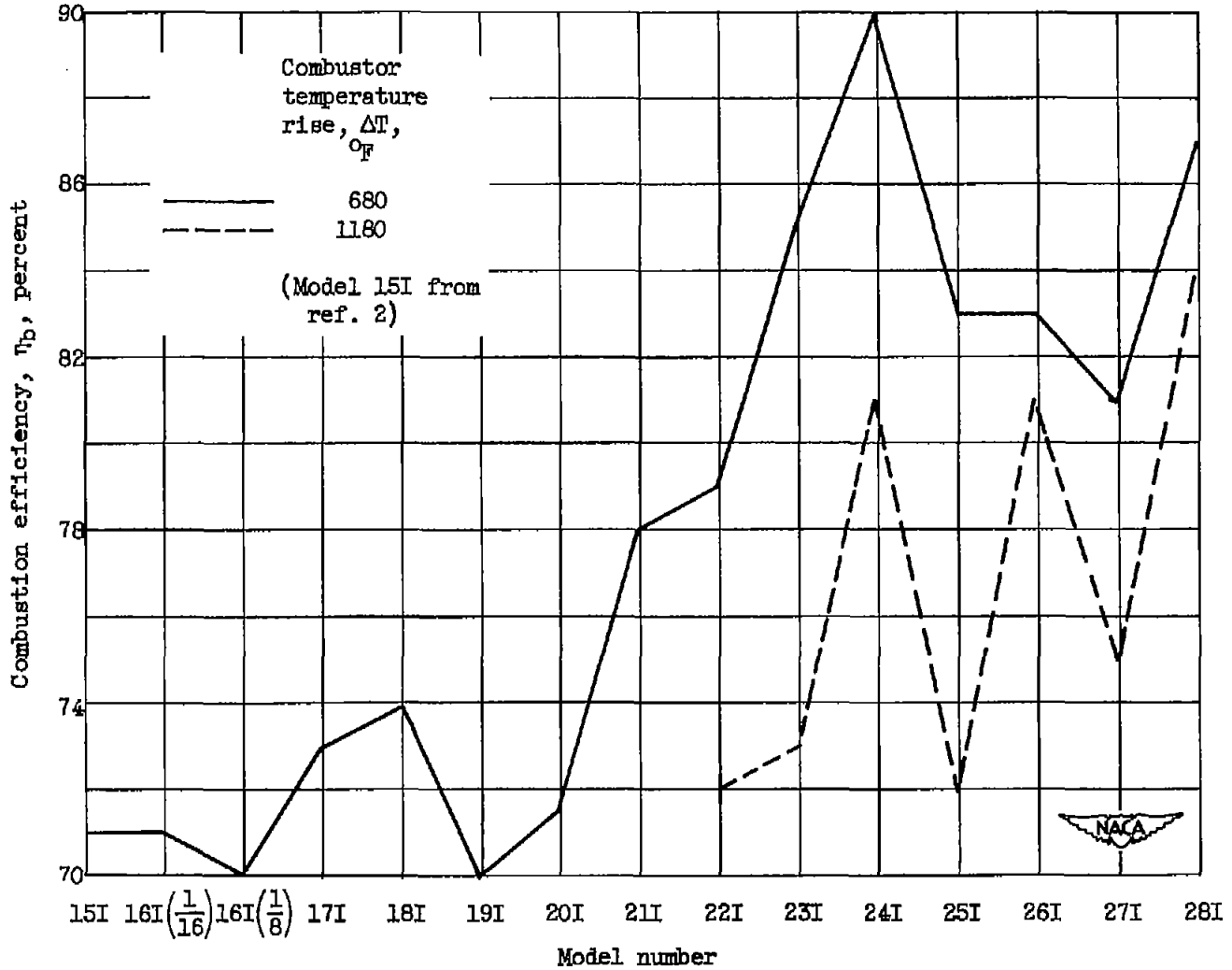

Figure 8. - Comparison of efficiencies of experimental combustors at test condition C for two values of combustor temperature rise.

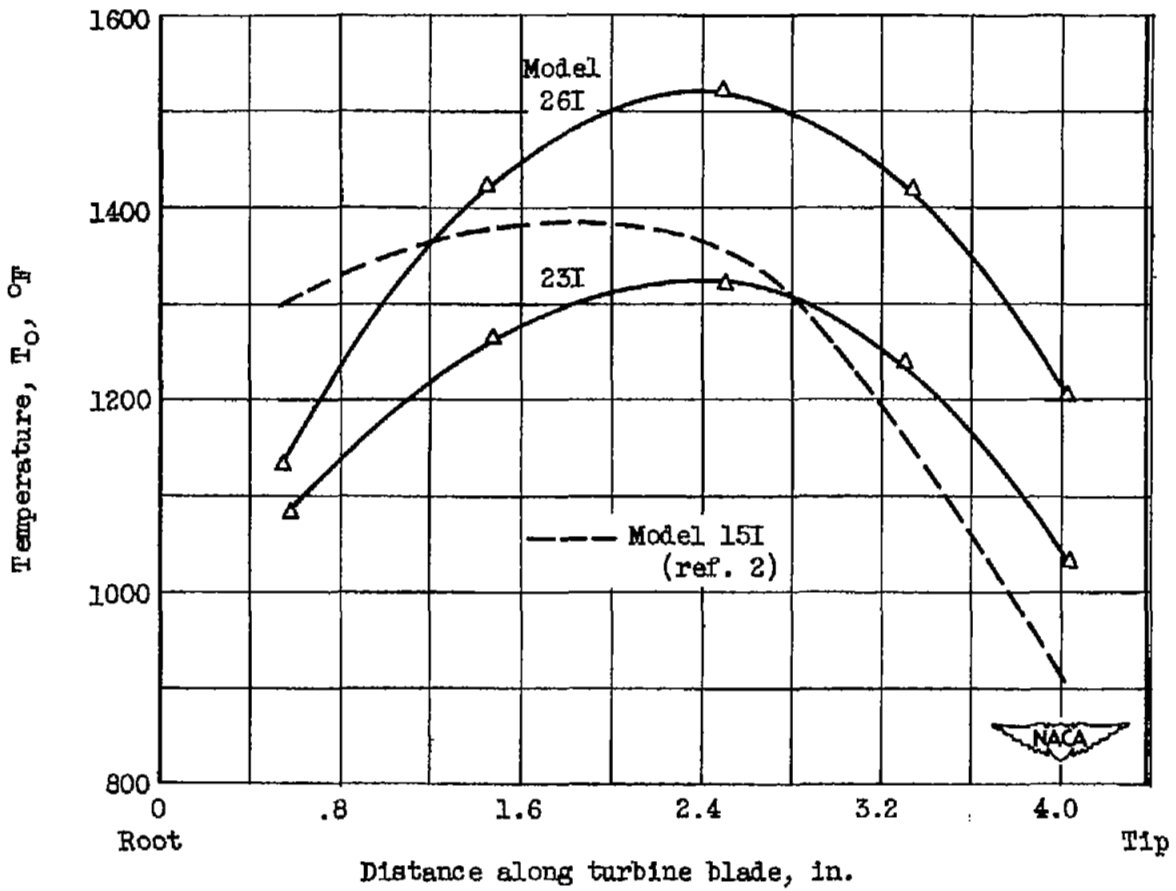

Figure 9. - Combustor-outlet radial temperature profiles at test condition C.

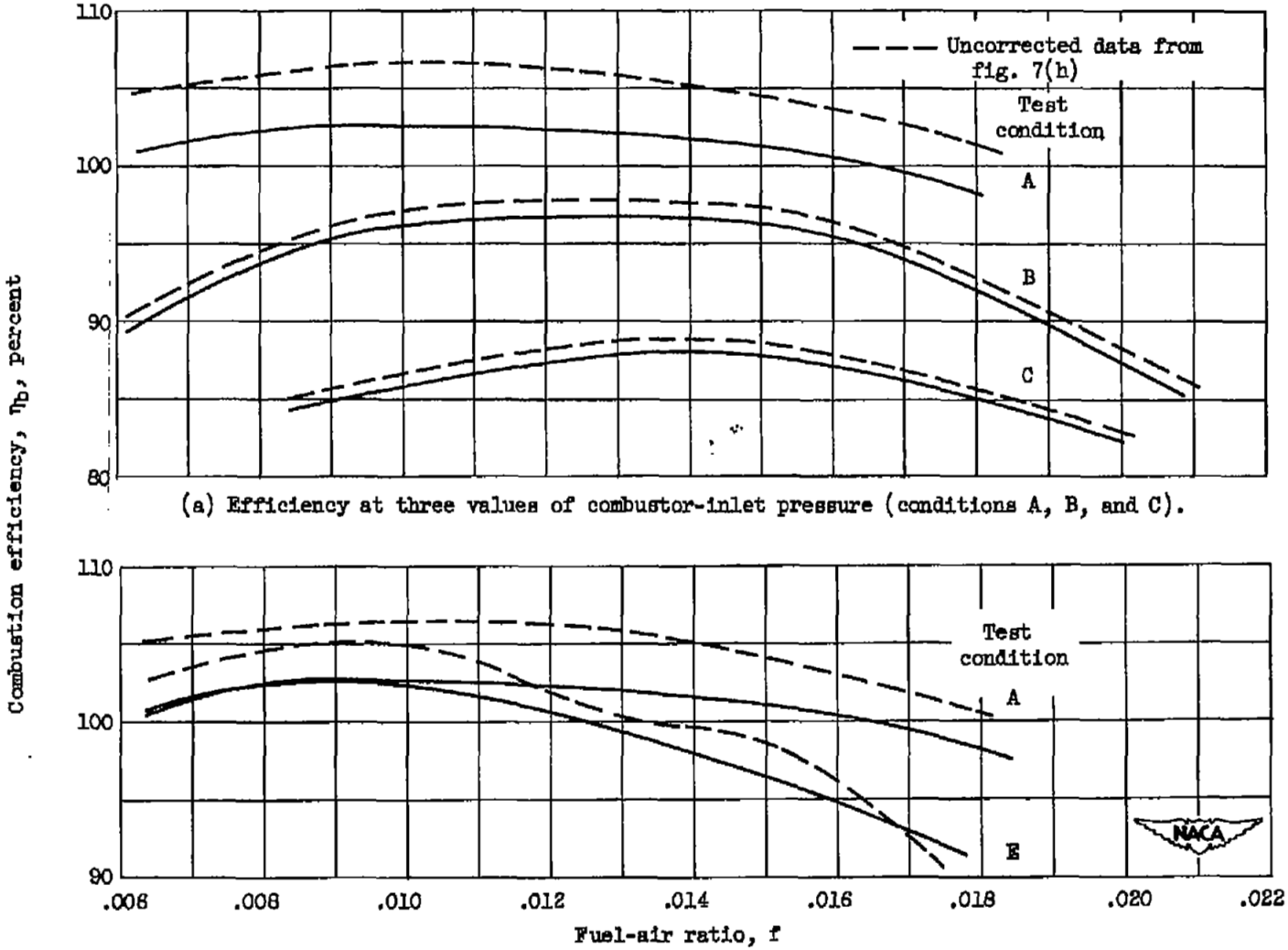

(a) Efficiency at three values of combustor-inlet pressure (conditions A, B, and C).

(b) Efficiency at two values of combustion air flow (conditions A and E).

Figure 10. - Combustion efficiency of model 28I combustor corrected for mass-flow distribution.

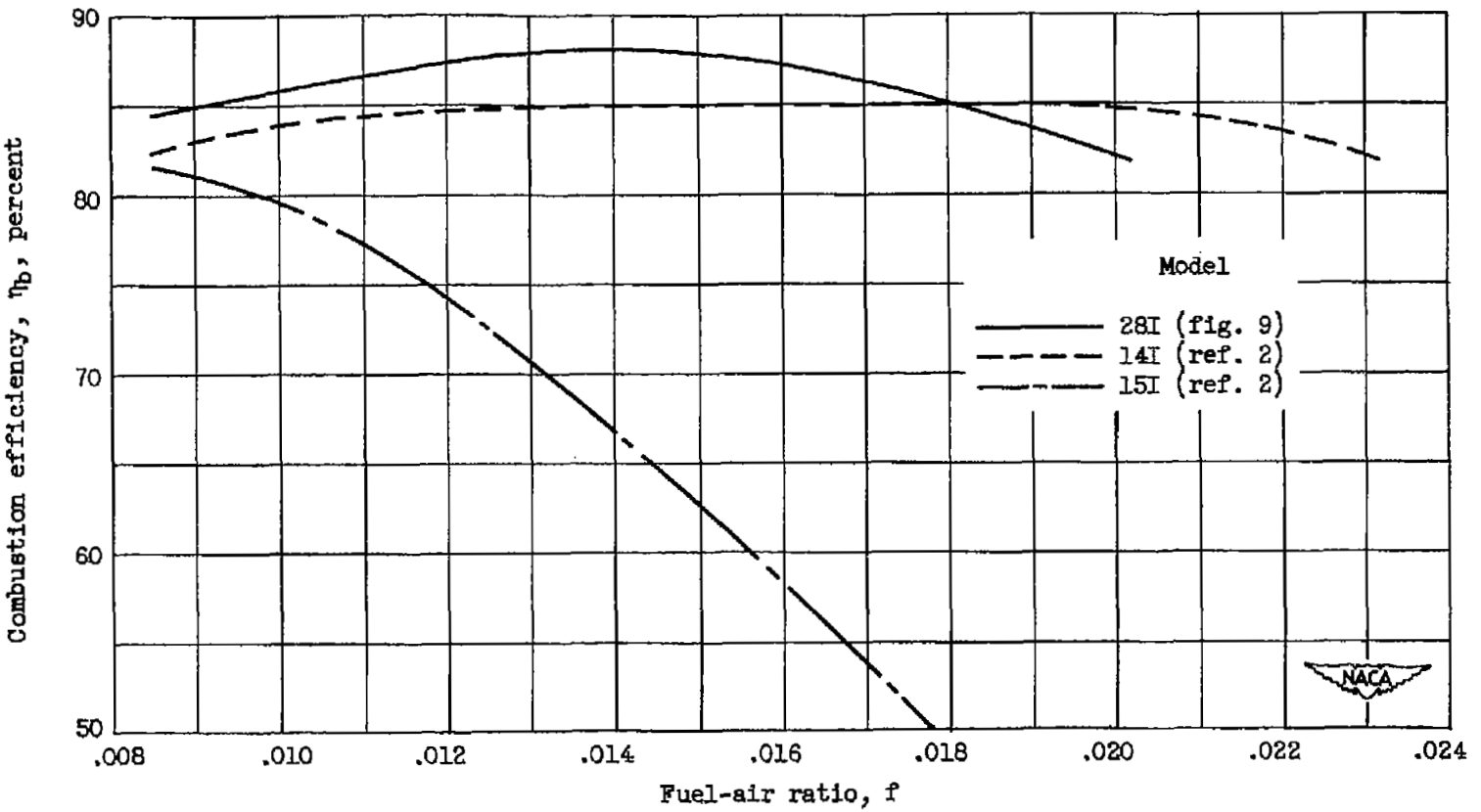

Figure 11. - Comparison of efficiency of model 28I combustor with that of models 14I and 15I at test condition C.

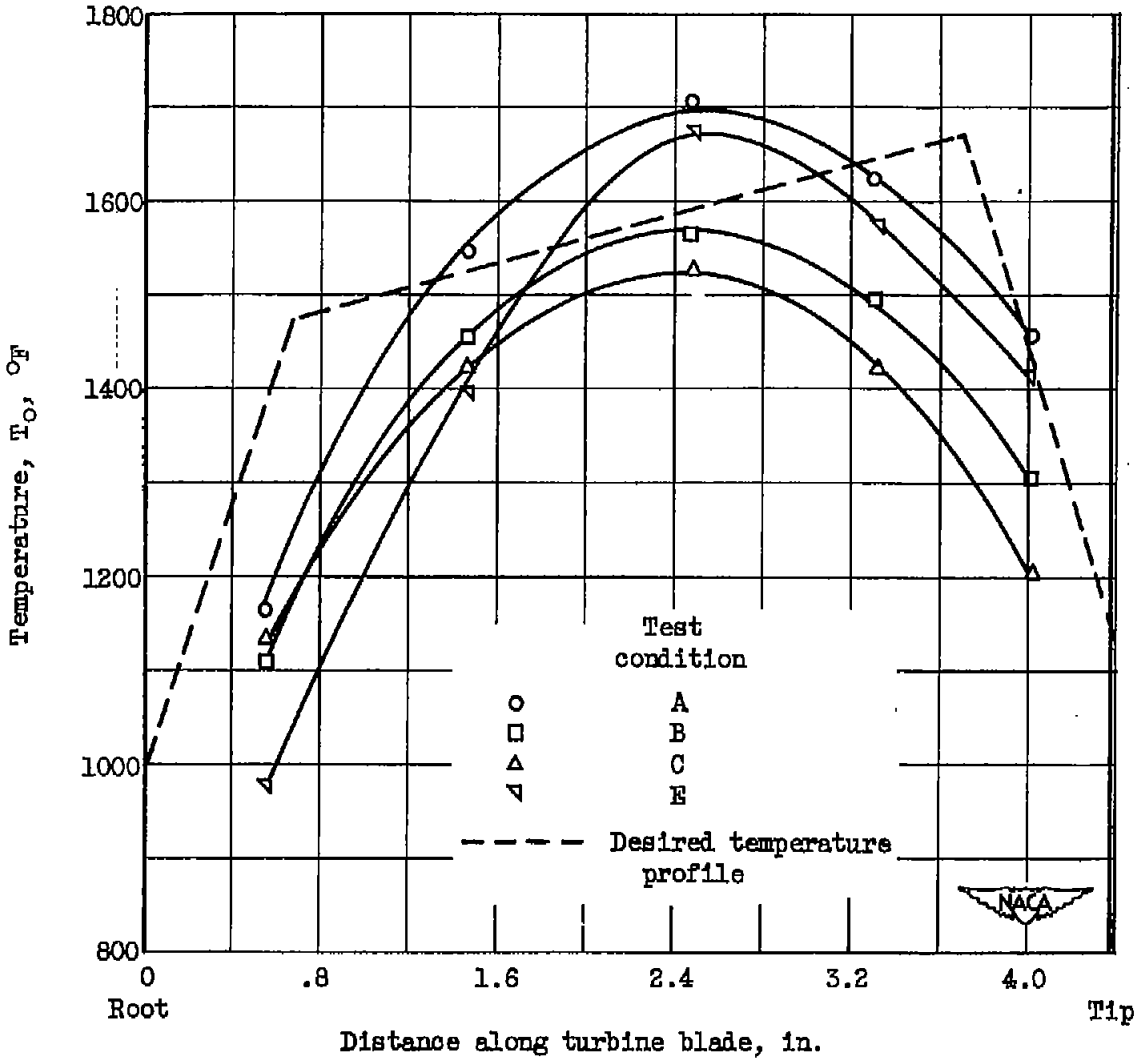

Figure 12. - Combustor-outlet radial temperature profiles for model 28I.

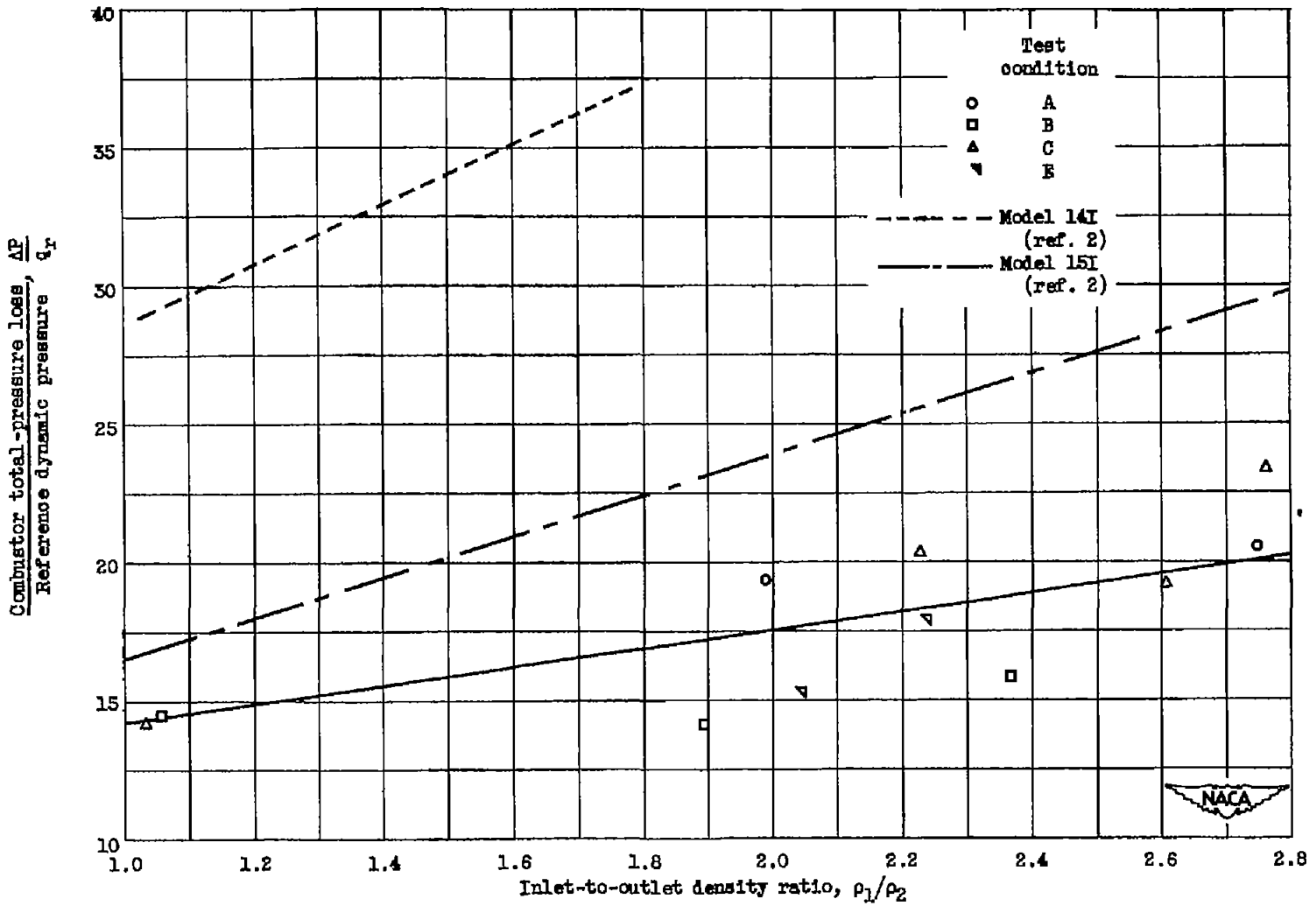

(a) Ratio of total-pressure loss to reference dynamic pressure loss.

Figure 13. - Combustor pressure losses of model 28I combustor.

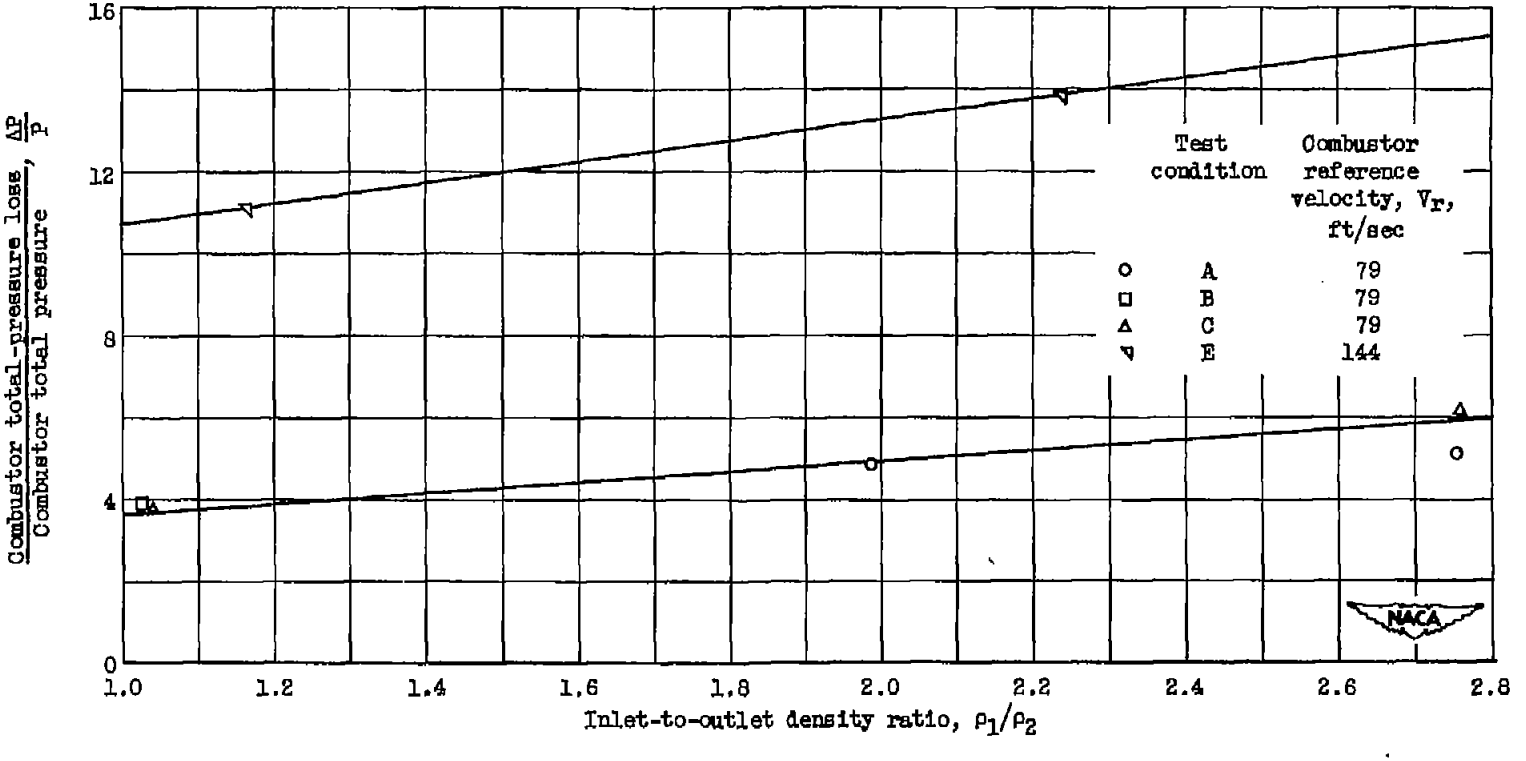

(b) Ratio of total-pressure loss to total inlet pressure.

Figure 13. - Concluded. Combustor pressure losses of model 28I combustor.

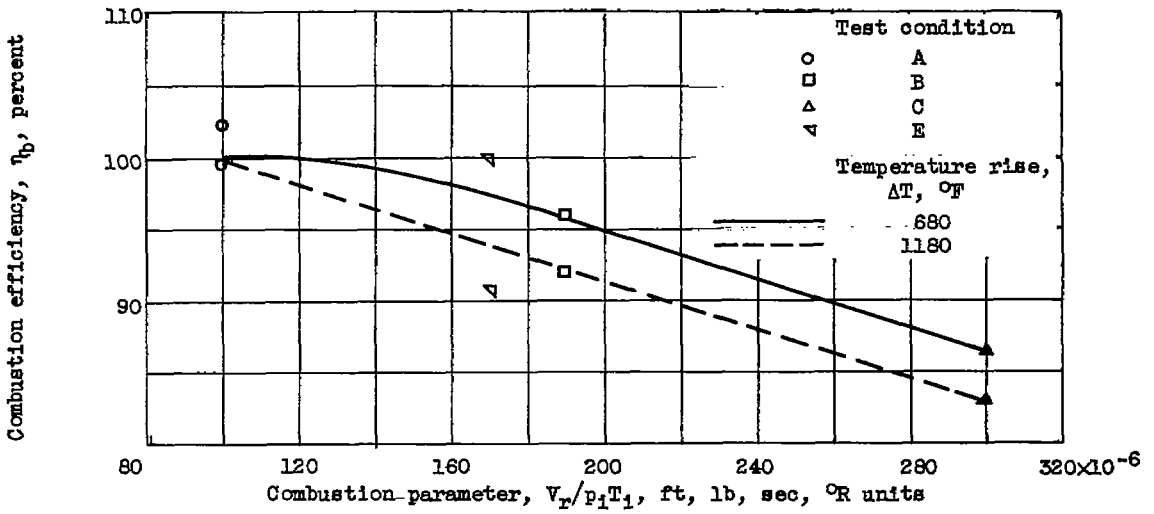

Figure 14. - Correlation of combustion-efficiency data of model 28I combustor with combustion parameter V_r/p_iT_i.

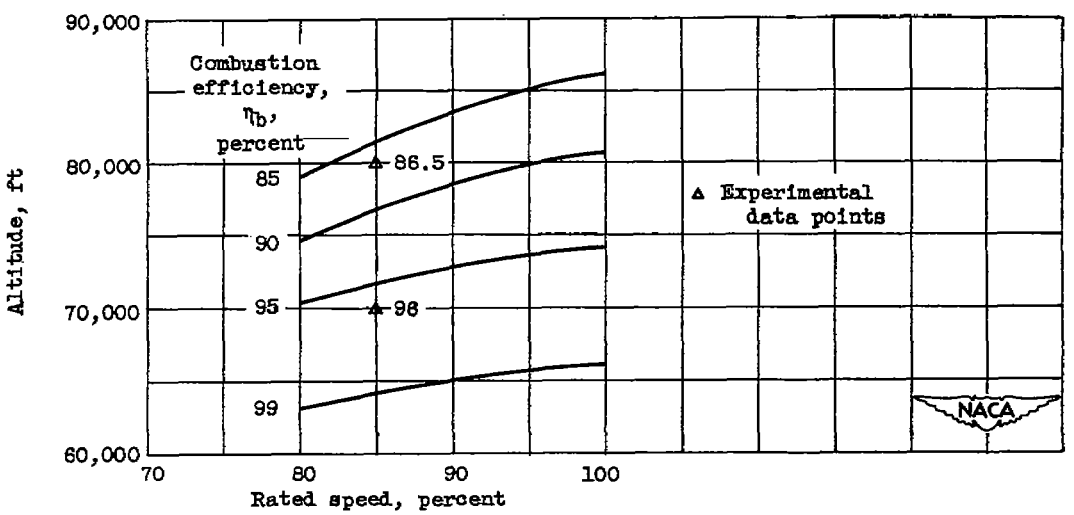

Figure 15. - Estimated flight performance of model 28I combustor in 5.2-pressure-ratio engine at flight Mach number of 0.6.

[redacted]